AB-INITIO RELATIVISTIC WAVEFUNCTIONS FOR DIATOMICS CONTAINING HEAVY ATOMS

by

Agustin Federico Ramos

B.Sc. Universidad Nacional Autonoma de Mexico, 1983

THESIS SUBMITTED IN PARTIAL FULFILLMENT OF

THE REQUIREMENTS FOR THE DEGREE OF

MASTER OF SCIENCE

in the Department

of

Chemistry

SIMON FRASER UNIVERSITY

January 1987.

APPROVAL

Name: Agustin F. Ramos

Degree: M.Sc.

Title of thesis: AB-INITIO RELATIVISTIC WAVEFUNCTIONS FOR DIATOMICS CONTAINING HEAVY ATOMS

Examining Committee:

Chairman: Prof. F.W.B. Einstein

Prof. G.L.Malli
Senior Supervisor

Prof. P.W.Percival

Prof. L.E.Ballentine

Prof. I.D.Gay
External Examiner
Department of Chemistry
Simon Fraser University, Burnaby, B.C.

Date Approved: Feb 12/87

PARTIAL COPYRIGHT LICENSE

I hereby grant to Simon Fraser University the right to lend my thesis, project or extended essay (the title of which is shown below) to users of the Simon Fraser University Library, and to make partial or single copies only for such users or in response to a request from the library of any other university, or other educational institution, on its own behalf or for one of its users. I further agree that permission for multiple copying of this work for scholarly purposes may be granted by me or the Dean of Graduate Studies. It is understood that copying or publication of this work for financial gain shall not be allowed without my written permission.

Title of Thesis/Project/Extended Essay

Ab-Initio Relativistic Wave Functions for Diatomics Containing Heavy Atoms

Author:

(signature)

AGUSTIN F. RAMOS

(name)

February 16, 1987

(date)

ABSTRACT

Recently, ab-initio four-component relativistic calculations for AuH have been reported by Malli and Pyper. It was concluded from these and from the relativistic calculations for Au_2, Bi_2, BiH and preliminary relativistic calculations for TlH that although the 5d orbitals are substantially involved in the bonding of gold compounds these do not participate in the bonding of TlH and bismuth compounds. Furthermore, they established that the non-relativistic calculation cannot explain either qualitatively or quantitatively the features of chemical bonding and properties of AuH as compared with the relativistic calculation which predicts a shorter bond length, a higher vibrational frequency and a doubling of the dissociation energy.

In order to compare the role of the 5d orbitals in the closed-shell compounds of hydrogen with the heavy elements Au to Bi, ab-initio relativistic wavefunctions and dissociation energies have been calculated for the species HgH^+, TlH and PbH^+ using the Relativistic Integrals Programme (RIP) developed at Cambridge. For comparison, to study the relativistic effects, the non-relativistic wavefunctions for these species and for BiH have also been calculated.

To complement this study, a computer programme developed here (using the numerical techniques of RIP) has been used to calculate the dipole moments and mass expectation values for the diatomics AuH, HgH^+, TlH, PbH^+ and BiH. Moreover, contour maps

of relativistic molecular orbitals (RMO) and their densities have been generated to present a visual appreciation of the electronic charge distributions in these systems.

It is found that the 5d orbitals also participate in the bonding of HgH^+ but these are unimportant for TlH and PbH^+. It is also found that the calculated relativistic and non-relativistic values of the dipole moments for these heavy diatomics significantly differ in magnitude and in some cases even in sign.

ACKNOWLEDGMENTS

I would like to express my gratitude to my supervisor, Professor G. L. Malli, for his encouragement and direction throughout the course of this work.

I am grateful to Dr. N. C. Pyper, for stimulating discussions and for providing me with the Relativistic Integrals Computer Programme (RIP).

Also, I would like to thank Professors L. E. Ballentine and P. Percival, for their helpful comments.

DEDICATION

To Elsa with love.

List of Tables.

Table

Page

Table of Contents.

List of Figures.

Figure

Page

1. INTRODUCTION

During the past decade there has been an increasing interest in the study of relativistic effects in atoms, molecules and solids [2].

In the case of atoms, the state of the art is such that accurate fully ab-initio relativistic calculations have been performed [3,4]. In the case of molecules, the first relativistic SCF formulation for closed-shell molecules was developed by Malli and Oreg [5]. However, all electron ab-initio relativistic calculations were only reported for the light systems Li_2 and Be_2 [6] for which the relativistic effects are unimportant. This was, in part, due to the fact that at that time, fully ab-initio relativistic calculations on molecular systems containing heavy atoms were prohibitively expensive in computer time.

In view of this, less rigorous but more practical methods have been devised to investigate the electronic structure of systems containing heavy atoms. Among them, there are : the one-centre expansion (OCE) method which has been applied only for hydrides [7,8]; the effective core potential (ECP) method which has been applied to diatomics and polyatomics containing heavy atoms [9,10,11]; and a perturbation approach that has been applied to hydrides and linear molecules containing heavy atoms [12,13]. However, it should be noted that the results reported from calculations on heavy systems using the last two methods are suspicious [14], since it is well known that even the

valence electrons of a heavy atom are significantly modified by relativity [44]. Thus, any molecular calculation treating the valence electrons should be based on a Dirac Hamiltonian as proposed by Ishikawa and Malli [15]. Moreover, it has been shown by Pyper and Marketos [16] that in a heavy atom, although the indirect effects of relativity are well described by first order perturbation theory, the direct effects are too large to be treated accurately.

More recently, a computer programme RIP (Relativistic Integrals Programme) was developed to perform fully relativistic calculations [17], using a method based on the Dirac equation for a diatomic system. It has been used by Malli and Pyper [1] to report the first fully relativistic ab-initio calculation for gold hydride (AuH). In this calculation the nature of the bonding in gold hydride was investigated, and it was found that, contrary to the naive concept that the bonding in gold hydride is fully described by the participation of only the 6s orbital of the gold atom and the 1s orbital of the hydrogen atom, there is also a significant participation of the 5d orbitals of gold manifested through 5d-6s hybridization in the valence molecular orbitals describing the bond. Furthermore, these bonding features have been shown to be due to relativity, since the non-relativistic limit calculations on AuH do not show 5d participation.

The above mentioned results on gold hydride provided the motivation to investigate, by using RIP, the bonding nature and

relativistic effects in the similar heavy systems HgH^+, TlH, PbH^+ and BiH, and compare their 5d-orbital participation in bonding. Moreover, to visualize the bonding characteristics and the 5d charge density redistribution in these systems, a computer programme was developed to perform orbital amplitude and charge density contour plots. Furthermore, to investigate the relativistic effects on properties other than the energy, another computer programme was developed to evaluate dipole moments by using the same numerical techniques as RIP.

2. METHOD

The theoretical methods for relativistic calculations on molecules have been fully described elsewhere [5,18]. With the exception of a detailed description of the methods and computational techniques used for the calculation of the dipole moment, the mass operator and the generation of contour plots, only a brief summary of the theory for calculating the wavefunction and total energy of a diatomic [19,20] will be given here. In particular, the methods will focus on diatomics of the form XH where X is a heavy atom or ion ($X=Hg^+$, Tl, Pb^+, Bi) and H is the hydrogen atom.

2.1 Wavefunction Construction.

Using the orbital approximation, i.e., with each electron described by a four-component function ϕ of only its space and spin coordinates called a relativistic molecular orbital (RMO), the N-electron approximate wavefunction Ψ_e is constructed as the Slater determinant (SD) of N RMOs as:

$$|\Psi_e\rangle = S\,\mathcal{A}\left\{\prod_{i=1}^{N} |\phi_i(i)\rangle\right\} \qquad (1)$$

where $\mathcal{A}$ is an antisymmetrizer and S is a normalization constant. For the RMOs, the relativistic analogue of the LCAO method [21] is used in which each RMO is expanded in terms of Dirac-Fock atomic orbitals (DFAOs) of the constituent species X and H. These DFAOs are readily computed using the Multi-Configuration Dirac-Fock (MCDF) programme [22], and have

the standard central field form [23]

$$|u_q \kappa m\rangle = \frac{1}{r_q}\begin{pmatrix} P_{\kappa}(r)\,\chi_{\kappa m}(\theta_q,\phi) \\ iQ_{\kappa}(r)\,\chi_{-\kappa m}(\theta_q,\phi)\end{pmatrix}, \qquad (2)$$

where (r_q,θ_q,ϕ) are the spherical coordinates (see figure 1) of the electron with respect to centre q (q=A,B). The $P_{\kappa}(r)$ and $Q_{\kappa}(r)$ are the large and the small (purely numerical) radial functions of the subshell [43] and $\chi_{\kappa m}(\theta_q,\phi)$ is a vector coupled space-spin function given by

$$\chi_{\kappa m}(\theta_q,\phi) = \sum_{m_s=-\frac{1}{2}}^{\frac{1}{2}} \langle \ell\tfrac{1}{2}(m-m_s)m_s|jm\rangle\, Y_{\ell,m-m_s}(\theta_q,\phi)\,|\tfrac{1}{2}\,m_s\rangle, \qquad (3)$$

where $Y_{\ell,m-m_s}(\theta_q,\phi)$ is a spherical harmonic (normalized such that $Y_{00}=\frac{1}{2\sqrt{\pi}}$), while $|\frac{1}{2}\pm m_s\rangle$ are the two component spin functions,

$$|\tfrac{1}{2}\tfrac{1}{2}\rangle \equiv |\alpha\rangle\,, \quad |\tfrac{1}{2}\tfrac{-1}{2}\rangle \equiv |\beta\rangle\,, \qquad (4)$$

The quantum number m takes half-integer values and is the eigenvalue of the operator $\hat{j}_z$ corresponding to the z-component of the total angular momentum $(\hat{\vec{j}}=\hat{\vec{\ell}}+\hat{\vec{s}})$. The quantum number κ, which can be a positive or a negative integer, defines both eigenvalues j and ℓ through

$$\kappa = -(j+\tfrac{1}{2})\,a, \qquad (5)$$

Figure 1. Diatomic Coordinate System.

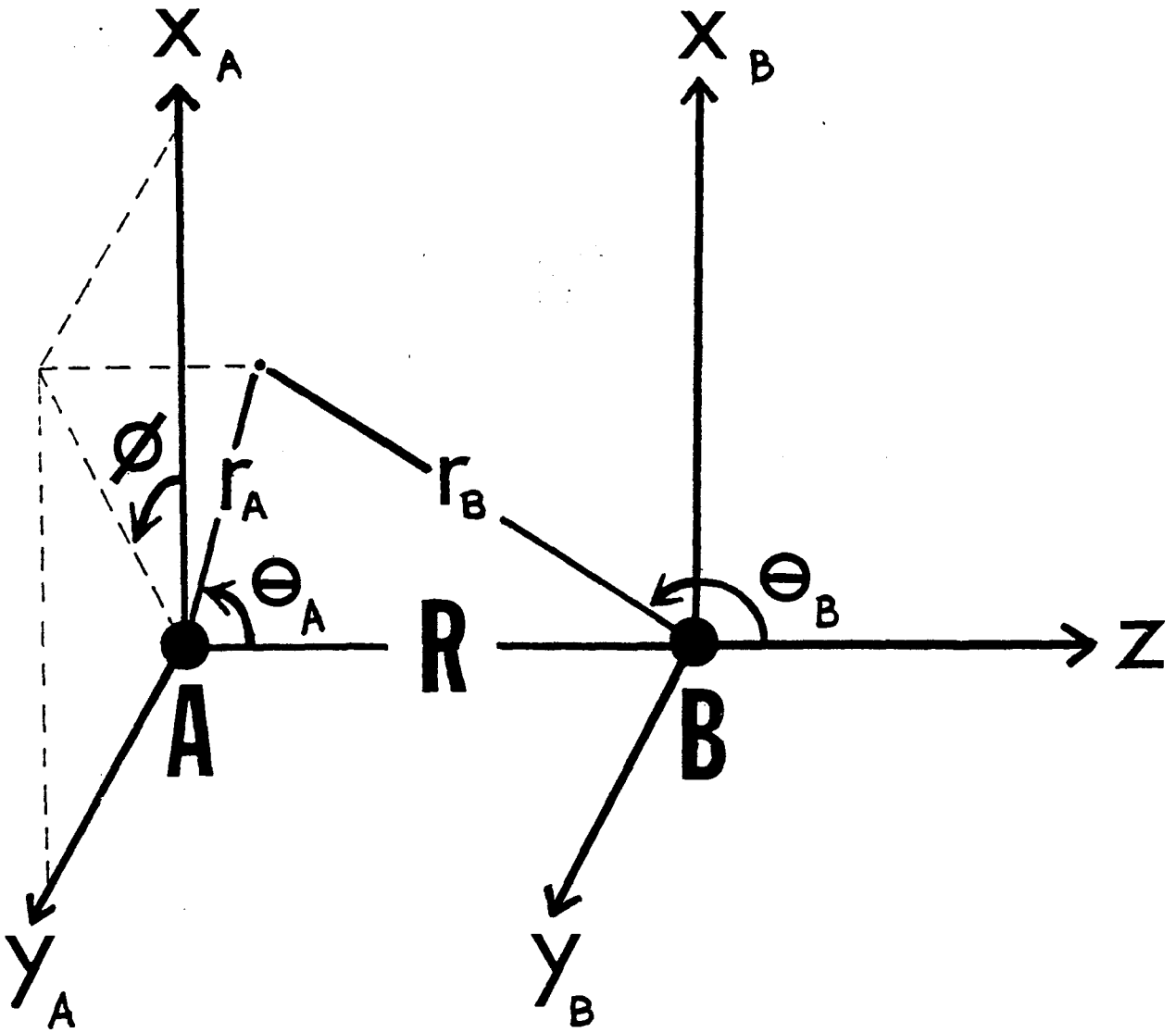
X A
X B
ø
r A
r B
θ A
θ B
R
A
B
Z
Y A
Y B

where $a=1$ $(a=-1)$ for $j = \ell + 1/2$ $(j = \ell - 1/2)$. To simplify the problem of finding the explicit form of all the N RMOs, the frozen core approximation is used, i.e., it is assumed that n_c inner electrons of X will remain unaffected upon molecule formation. A core wavefunction Φ_c is taken as a SD of RMOs, where each RMO is uniquely represented by one inner DFAO of X,

$$|\Phi_c(\vec{r}_1,..,\vec{r}_{n_c})\rangle = \mathcal{A}\left\{\prod_{i=1}^{n_c} |u_{q,i}(\vec{r}_{q,i})\rangle\right\}, \tag{6}$$

while for the remaining $N-n_c$ valence electrons the wavefunction Φ_v is taken to be of the form :

$$|\Phi_v(\vec{r}_{n_c+1},..,\vec{r}_N)\rangle = \mathcal{A}\left\{\prod_{i=n_c+1}^{N} |\phi_i(i)\rangle\right\} . \tag{7}$$

The Φ_v, describes both those electrons occupying open subshells of X and H and those occupying closed subshells of X that are significantly affected by the formation of the molecule. In this frozen core approximation, the total electronic wavefunction Ψ_e then takes the form [1],

$$|\Psi_e\rangle = S\mathcal{A}'\left\{|\Phi_c(\vec{r}_1,..,\vec{r}_{n_c})\rangle|\Phi_v(\vec{r}_{n_c+1},..,\vec{r}_N)\rangle\right\}, \tag{8}$$

where $\mathcal{A}'$ is a partial anti-symmetrizer which only interchanges coordinates between the sets $\{\vec{r}_1,..,\vec{r}_{n_c}\}$ and $\{\vec{r}_{n_c+1},..,\vec{r}_N\}$.

Furthermore, to ensure the strong orthogonality between Φ_c and Φ_v [17], the basis set $\{|u_i\rangle\}$ of valence DFAOs is

Schmidt-orthogonalized against all the core DFAOs defining a core-orthogonal basis $\{[u_i' >\}$ with

$$|u_i'> = \sum_{j=1}^{N} T_{ji} |u_j> \quad . \tag{9}$$

In eq. 9, $[T]$ is the expansion coefficient matrix of the new basis $\{[u_i' >\}$ in terms of the core and the original valence orbitals $\{[u_i >\}$. In particular for the systems HX with H located at A and X located at B (see figure 1), only the hydrogen 1s DFAO gets orthogonalized against the core of X as

$$|u_{1s}'> = S_{1s} \left\{ |u_{A,1s}> - \sum_{i=1}^{n_c} <u_{B,i}|u_{A,1s}> |u_{B,i}> \right\} , \tag{10}$$

where S_{1s} is a normalization constant.

The expansion of the valence RMOs is then given in terms of the core-orthogonal basis $\{[u_i' >\}$ (defined in eq. 9),

$$|\phi_i> = \sum_{j=n_c+1}^{N} C_{ji} |u_j'> , \tag{11}$$

where $[C]$ is the coefficient matrix to be determined by an SCF procedure [21].

2.2 Molecular Energy.

With a wavefunction Ψ_e constructed in terms of DFAOs that are "electron-like" solutions (purely numerical) of the

Dirac-Fock equations for each of the constituent species makes unnecessary the use of projection operators onto an electron-like subspace [24,25] in evaluating the expectation value of the electronic energy E_e . Thus,

$$E_e(R) = \langle \Psi_e | \hat{\mathcal{H}}_e^N | \Psi_e \rangle , \qquad (12)$$

where R is the internuclear separation of the diatomic (see figure 1) and $\hat{\mathcal{H}}_e^N$ is the Dirac-Coulomb operator for the N-electron diatomic, given in atomic units ($\hbar$=1, m=1, e=1) by

$$\hat{\mathcal{H}}_e^N = \sum_{i=1}^{N} \left\{ c\, \hat{\vec{\alpha}}(i) \cdot \hat{\vec{p}}(i) + c^2 (\hat{\beta}(i) - \hat{1}) - Z_A \hat{r}_{Ai}^{-1} - Z_B \hat{r}_{Bi}^{-1} \right\} + \sum_{i<j} \hat{r}_{ij}^{-1} \qquad (13)$$

where $\hat{\vec{p}}$ is the operator for linear momentum, c is the velocity of light and $\hat{\vec{\alpha}}$ and $\hat{\beta}$ are the Dirac 4x4 matrices defined as

$$\hat{\vec{\alpha}} = \begin{pmatrix} 0 & \hat{\vec{\sigma}} \\ \hat{\vec{\sigma}} & 0 \end{pmatrix} , \qquad \hat{\beta} = \begin{pmatrix} I & 0 \\ 0 & -I \end{pmatrix} , \qquad (14)$$

where $\hat{\vec{\sigma}}$ are the 2x2 Pauli spin matrices and I is a 2x2 identity matrix. In eq. 13, Z_q (q =A,B) is the charge of nucleus q and $\vec{r}_{qi}$ is the vector distance of centre q to electron i (see figure 1).

From eq. 8 and due to the strong orthogonality between Φ_c and Φ_v , the total molecular energy E(R) (including the internuclear repulsion) can be decomposed into core and valence contributions [17,26]

$$E(R) = E_c(R) + E_v(R), \tag{15}$$

where $E_c(R)$ is given by

$$E_c(R) = \langle \Phi_c | \mathcal{H}_e^{n_c} | \Phi_c \rangle + \frac{Z_A Z_B}{R}, \tag{16}$$

and $E_v(R)$ is given by

$$E_v(R) = \langle \Phi_v | \hat{\mathcal{H}}_e^{N-n_c} + \sum_{i=n_c+1}^{N} \hat{V}_c(r_{Bi}) | \Phi_v \rangle . \tag{17}$$

In eq. 17, $\hat{V}_c(r_{Bi})$ is a one-electron operator containing all the direct and exchange interactions of valence electron i with the core of X located at B.

All the one-centre and two-centre integrals needed for the evaluation of $E_c(R)$ and $E_v(R)$ are readily computed using the Relativistic Integrals Programme (RIP) [19,20]. The minimization of $E_v(R)$ leads to the standard matrix eigenvalue problem [21]

$$[F][C] = [S][C][\epsilon], \tag{18}$$

where $[S]$ is the overlap matrix with elements $\langle u_i' | u_j' \rangle$, $[C]$ is the coefficient matrix defined in eq. 11, $[\epsilon]$ is the eigenvalue matrix and $[F]$ is the matrix of the one-electron Dirac-Fock operator with elements

$$F_{ij} = \langle u_i' | \hat{f} + \hat{J} - \hat{K} | u_j' \rangle , \tag{19}$$

with

$$\hat{f}(1) = c\hat{\vec{\alpha}}(1)\cdot\hat{\vec{p}}(1) + c^2(\hat{\beta}(1)-\hat{1}) - Z_A\hat{r}_{A1}^{-1} - Z_B\hat{r}_{B1}^{-1} + \hat{V}_c(r_{B1}) \,. \qquad (20)$$

In eq. 19, the coulomb ($\hat{J}$) and exchange ($\hat{K}$) operators are given as follows : [27]

$$\hat{J}(1) = \sum_{l=n_c+1}^{N} \int \frac{\phi_l^{\dagger}(2)\,\phi_l(2)}{r_{12}}\, d\tau_2 \,, \qquad (21)$$

$$\hat{K}(1)\,|\phi_j(1)\rangle = \sum_{l=n_c+1}^{N} |\phi_l(1)\rangle \int \frac{\phi_l^{\dagger}(2)\,\phi_j(2)}{r_{12}}\, d\tau_2 \,, \qquad (22)$$

where $\phi_l^{\dagger}$ stands for the Hermitian conjugate of ϕ_l .

Using an SCF procedure [21], eq. 18 is solved for E_v and [C] , whence the total molecular energy $E(R)$ and the approximate wavefunction $\Psi_e(R)$ are determined.

The dissociation energy, De, defined positive for a bound system, is given by the difference between the molecular energy for $R\rightarrow\infty$ (separated atoms) and that at R=Re (equilibrium position of the molecule). By virtue of the energy partition given in eq. 15, De is calculated as

$$D_e = E_{A,v} + E_{B,v} - \Delta E_c(R_e) + E_v(R_e) \,. \qquad (23)$$

In eq. 23, $E_{A,V}$ and $E_{B,V}$ are the energies of the valence electrons in the isolated atoms A and B, respectively and $\Delta E_c(R_e)$, which includes the nuclear-nuclear repulsion, is the difference between the energy of the core in the molecule and that of the same core in the isolated atoms [1].

2.3 Symmetry Considerations

The heteronuclear systems under study belong to the $C_{\infty v}$ double group.

Refering to the coordinate system of figure 1., some of the spatial operations included in $C_{\infty v}$ are [28] :

C_ϕ , for a rotation by ϕ around the z-axis,

H_{ys} , for a reflection in the plane y=0

(changing ϕ to $-\phi$)

The operators corresponding to these are given by [28] :

$$\hat{T}_\varphi = e^{-i\varphi \hat{J}_z} \tag{24}$$

and

$$\hat{T}_y = \hat{I}_D e^{-i\pi \hat{J}_y} \tag{25}$$

where $\hat{I}_D = \hat{\beta}\hat{I}_S$ [20] is the "Dirac inversion operator" corresponding to the spatial inversion ($\hat{I}_S$) changing r to -r.

It can be shown that the Dirac-Fock operator $\hat{F}$ (eqs. 18 and 19) is totally symmetric with respect to the symmetry

operations of the group $C_{\infty v}$ [20]:

$$[\hat{F}, \hat{T}_\varphi] = [\hat{F}, \hat{T}_y] = 0, \tag{26}$$

where the first commutation relation follows from the commutation of $\hat{F}$ with $\hat{J}_z$. However, since $\hat{T}_\varphi$ and $\hat{T}_y$ do not commute with each other, the eigenfunctions $|\phi_i\rangle$ of $\hat{F}$ cannot be simultaneous eigenfunctions of $\hat{F}$, $\hat{T}_\varphi$ and $\hat{T}_y$ but they can be for $\hat{F}$ and $\hat{T}_y$ or $\hat{F}$ and $\hat{T}_\varphi$. Choosing the latter option the eigenfunctions $|\phi_i\rangle$ are labeled as $|\phi_i\, m\rangle$, such that :

$$\hat{F}\,|\phi_i\, m\rangle = \epsilon_i\,|\phi_i\, m\rangle \tag{27}$$

$$\hat{J}_z\,|\phi_i\, m\rangle = m\,|\phi_i\, m\rangle \ . \tag{28}$$

Furthermore, it follows [18,28] that,

$$\hat{F}\,(\hat{T}_y\,|\phi_i\, m\rangle) = \epsilon_i\,(\hat{T}_y\,|\phi_i\, m\rangle) \tag{29}$$

$$\hat{J}_z\,(\hat{T}_y\,|\phi_i\, m\rangle) = -m\,(\hat{T}_y\,|\phi_i\, m\rangle) \tag{30}$$

and thus, the energy levels are doubly degenerate [18,28] and the ket $(\hat{T}_y\,|\phi\, m\rangle)$ differs from the ket $(|\phi\, -m\rangle)$ by at most a phase factor $e^{i\delta}$ [18,28]

$$\hat{T}_y\,|\phi\, m\rangle = e^{i\delta}\,|\phi\, -m\rangle \tag{31}$$

In connection with the evaluation of the matrix elements F_{ij} of eq. 19, it follows [18,28] from eqs. 28 and 31 that

$$F_{ij} = \langle u_i' m | \hat{F} | u_j' m' \rangle \delta_{mm'} \tag{32}$$

$$\langle u_i' m | \hat{F} | u_j' m \rangle = \langle u_i' -m | \hat{F} | u_j' -m \rangle \, . \tag{33}$$

Thus, the matrix [F] is blocked by m-value and only the positive m-value blocks need to be calculated.

2.4 Dipole Moment.

In a coordinate system with origin at centre A and z-axis pointing towards centre B (see figure 1), the expectation value of the dipole moment in atomic units (a. u.) is given by [42]

$$\langle \hat{\vec{\mu}}_A \rangle = Z_B \vec{R}_{AB} - \langle \Psi_e | \sum_{i=1}^{N} \hat{\vec{r}}_A(i) | \Psi_e \rangle \, . \tag{34}$$

The first term in eq. 34 is the nuclear contribution to the dipole given by centre B of nuclear charge Z_B located at a distance R_{AB} from A. The second term is the electronic part of the dipole due to the N electrons of the system.

The vector operator $\hat{\vec{r}}_A(i)$ for the position of electron i with respect to centre A can be decomposed into its $\hat{x}_A(i)$, $\hat{y}_A(i)$ and $\hat{z}_A(i)$ components; however, only the z-component will have a

non-zero contribution to the dipole moment because due to the axial symmetry of the diatomic, the contributions from the x and y components vanish.

This can be seen by using the operator $\hat{T}_{\pi,T}$, defined as

$$\hat{T}_{\pi,T} = \prod_{i=1}^{N} \hat{T}_{\pi}(i) \tag{35}$$

that corresponds to the N-electron generalization of the operator for a rotation by π in the z-axis and satisfies

$$\hat{T}_{\pi,T} |\Psi_e M\rangle = e^{-i\pi M} |\Psi_e M\rangle \tag{36}$$

$$\hat{T}_{\pi,T}^{-1} \left(\sum_{i=1}^{N} \hat{q}(i) \right) \hat{T}_{\pi,T} = - \sum_{i=1}^{N} \hat{q}(i) , \quad (q=x,y), \tag{37}$$

Thus,

$$\begin{aligned} \langle \Psi_e M | \sum_{i=1}^{N} \hat{q}(i) | \Psi_e M \rangle &= \langle \Psi_e M | \hat{T}_{\pi,T}^{+} \hat{T}_{\pi,T} \sum_{i=1}^{N} \hat{q}(i) | \Psi_e M \rangle \\ &= - \langle \Psi_e M | \sum_{i=1}^{N} \hat{q}(i) | \Psi_e M \rangle \qquad (38) \\ &= 0 \ . \end{aligned}$$

Therefore, the electronic contribution to the dipole μ_A^e is given only by the expectation value of

$$\mu_A^e = \langle \Psi_e | \sum_{i=1}^{N} \hat{z}_A(i) | \Psi_e \rangle \ . \tag{39}$$

By substituting Ψ_e from eq. 8 into the above relation, μ_A^e gets the molecular orbital approximation form, with contributions from the n_c RMOs formed by pure DFAOs of X, each having a centroid of charge at R units from A that make up a core dipole

$$\mu_{A,C}^e = \sum_{i=1}^{n_c} \langle u_{i,B}\, Km \,|\, \hat{z}_A \,|\, u_{i,B}\, Km \rangle = n_c R , \tag{40}$$

and from the $(N - n_c)$ valence RMOs that make up the valence dipole

$$\mu_{A,V}^e = \sum_{i=n_c+1}^{N} \langle \phi_i \,|\, \hat{z}_A \,|\, \phi_i \rangle . \tag{41}$$

Thus,

$$\mu_A^e = n_c R + \mu_{A,V}^e \tag{42}$$

The valence dipole moment is further simplified by symmetry by noting that $[\hat{z}_A, \hat{T}_\varphi] = [\hat{z}_A, \hat{T}_\gamma] = 0$, then

$$\mu_{A,V}^e = 2 \sum_{m>0} \sum_{i=ncm}^{Nvm} \langle \phi_i\, m \,|\, \hat{z}_A \,|\, \phi_i\, m \rangle = 2 \sum_{m>0} \sum_{i=ncm}^{Nvm} [Z_A^{RMO}]_{ii}^m \tag{43}$$

where $[Z_A^{RMO}]^m$ is the molecular dipole m-submatrix, ncm is the number of core orbitals having an m-value and Nvm is the number

of the valence orbitals with that m-value. The elements of these submatrices are readily given in terms of the original DFAOs by making use of the transformations $[T]$ (eq. 9) and $[C]$ (eq. 11) as

$$[Z_A^{RMO}]^m_{ij} = \sum_{pqlk} [C]^m_{pi} [T]^m_{qp} [Z_A^{DFAO}]^m_{qk} [T]^m_{kl} [C]^m_{lj} = [(TC)^\dagger Z_A^{DFAO} TC]^m_{ij} \quad (44)$$

where $[Z_A^{DFAO}]^m$ is the m-submatrix of the electric dipole in the DFAO basis.

From eqs. 34, 43 and 44, the total dipole moment is given by

$$\langle \hat{\mu}_A \rangle = (Z_B - n_c) R - 2 \sum_{m>0} \sum_{i=ncm}^{Nvm} [(TC)^\dagger Z_A^{DFAO} TC]^m_{ij} \quad (45)$$

Clearly, the only quantities needed to evaluate (45) are the $[Z_A^{DFAO}]^m_{ij}$ matrix elements since the $[C]$ and $[T]$ matrices are determined when the total energy $E(R)$ is calculated through the SCF procedure. These matrix elements can be one-centre or two-centre integrals having the form

$$[Z_A^{DFAO}]^m_{qq'} = \langle u_{q,c(q)}^{K(q)\,m} | \hat{Z}_A | u_{q',c(q')}^{K(q')\,m'} \rangle \quad (46)$$

In the case that the DFAOs are centered on the same centre (c(q)=c(q')=c), each one-centre integral (4 bits in principle) is reduced to only one radial integration as (see appendix 1)

$$\langle u_{q,c}\kappa m|\hat{Z}_A|u_{q',c}\kappa' m'\rangle = d^1(m,m',j,j')\int_0^\infty (PP'+QQ')r_c dr_c + R\delta_{qq'}\delta_{cB} \quad (47)$$

where d^1 is an angular coefficient [41] and the radial integration is done numerically using the methods of the MCDF [22] programme.

When the DFAOs are not centered on the same centre (two-centre integrals), unfortunately there is no angular simplification for the Θ integration and each two-centre integral will produce four overlap type integrals of the form

$$I_d = \int \frac{F(r_A)}{r_A} Y^*_{lm}(\theta_A,\phi)\ \frac{F(r_B)}{r_B} Y_{l'm'}(\theta_B,\phi)\, r_A \cos\theta_A\, d\tau. \quad (48)$$

Following the numerical methods of RIP [20] (see appendix 2), each I_d integral is calculated using a 24x24 Gauss quadrature [29].

2.5 Mass Operator.

Defining the total mass operator $\hat{M}$ of the N-electron system as [30]

$$\hat{M} = \sum_{i=1}^{N} c^2(\hat{\beta}(i) - \hat{1}), \quad (49)$$

where the rest mass energy of each electron has been subtracted such that the zero of energy corresponds to that of the free electron, the expectation value of $\hat{M}$ is given by

$$\langle \hat{M} \rangle = \langle \Psi_e | \hat{M} | \Psi_e \rangle = \sum_{i=1}^{N} \langle \phi_i | c^2(\hat{\beta}(i) - \hat{1}) | \phi_i \rangle . \qquad (50)$$

By virtue of the symmetry of the problem and using the same arguments as those given for the dipole moment, the expectation value of $\hat{M}$ in terms of the original DFAOs is

$$\langle \hat{M} \rangle = 2 \sum_{m>0} \sum_{i=1}^{N/2} [(TC)^{\dagger} M^{DFAO} TC]^{m}_{ii} , \qquad (51)$$

where $[M^{DFAO}]^{m}_{ij}$ is the m-submatrix of the mass operator in terms of the original DFAO basis and has elements

$$[M^{DFAO}]^{m}_{ij} = \langle u_{i,c(i)}{}^{\kappa(i) m} | c^2(\hat{\beta} - \hat{1}) | u_{j,c(j)}{}^{\kappa(j) m} \rangle , \qquad (52)$$

which can be one-centre (c(i)=c(j)) or two-centre (c(i)≠c(j)). For the one-centre type integrals, the central field symmetry of the DFAOs simplifies the integration to a radial integral [23] of only the small components that is evaluated with the MCDF [22] numerical methods,

$$\langle u_{s,c}{}^{\kappa m} | c^2(\hat{\beta} - \hat{1}) | u_{t,c}{}^{\kappa' m'} \rangle = -2 \delta_{jj'} \delta_{mm'} \delta_{aa'} c^2 \int_0^{\infty} QQ' dr_c \qquad (53)$$

For each two-centre integral, the two overlap-type integrals over the small components have the form

$$I_M = \int \frac{Q(r_A)}{r_A} Y^*_{\ell m}(\theta_A,\phi) \frac{Q'(r_B)}{r_B} Y_{\ell' m}(\theta_B,\phi)\, d\tau, \qquad (54)$$

and these are calculated using the same numerical methods as for the evaluation of the dipole moment (see appendix 2).

The expectation value of the total mass operator is evaluated in order to check the relativistic virial ratio [30],

$$\frac{\langle E \rangle}{\langle M \rangle} = 1 , \qquad (55)$$

which is satisfied at R=Re for the wavefunction that minimizes the total energy E of the system.

2.6 Contour Plots.

2.6.1 RMO Contour Plots.

In the XZ-plane (see figure 1), the RMO constant amplitude contour line of the ith component of the jth RMO $\phi_j(\vec{r})$ is given by

$$\phi^i_j(x,0,z) = A \qquad (56)$$

where A is the amplitude constant value. From eqs. 9 and 11, this expression is given in terms of the original DFAOs $u_s(\vec{r})$ as

$$\phi^i_j(x,0,z) = \sum_{sr} T_{sr} C_{rj} u^i_s(x,0,z) = A \qquad (57)$$

The form of each $u^i_{s,p}$ centered at p (p=A or B) is known and is given in general by

$$u^i_{s,p} = b\,\frac{f(r_p)}{r_p}\,P_\ell(\cos\theta_p)\,, \tag{58}$$

where b is a constant (that depends on the quantum numbers of DFAO $u_{s,p}$), $f(r_p)$ is a purely numerical radial function (calculated with the MCDF programme) and $P_\ell(\cos\theta_p)$ is a Legendre polynomial.

2.6.2 $\Delta\rho_{5d}$ Contour Plot.

The electronic charge density function ρ derived from the wavefunction Ψ_e is given in the orbital approximation by [31]

$$\rho(\vec{r}) = \sum_{j=1}^{N} \phi_j^{\dagger}(\vec{r})\,\phi_j(\vec{r})\,, \tag{59}$$

where

$$\phi_j^{\dagger}(\vec{r})\,\phi_j(\vec{r}) = \sum_{i=1}^{4} \phi_j^{i*}(\vec{r})\;\phi_j^{i}(\vec{r}) \tag{60}$$

is the contribution of the four components of the ϕ_j RMO to the density.

In the plane XZ, where the contour lines are defined,

$$\rho(x,0,z) = \sum_{j=1}^{N}\sum_{i=1}^{4} \left[\,\phi_j^{i}(x,0,z)\right]^2\,. \tag{61}$$

Within the frozen-core approximation, according to the core size defined for the calculation (n_c in eq. 6), different wavefunctions will be constructed showing different electronic molecular densities. In particular for the XH systems under study, it is desirable to visualize the change in charge density that each system undergoes when the $5\bar{d}$ and 5d DFAOs of X are included in the core wavefunction or not. This difference can be visualized by forming the difference density plot $\Delta\rho_{5d}$ given by

$$\Delta\rho_{5d} = \rho' - \rho'' \tag{62}$$

where ρ' and ρ'', refer to the charge densities obtained from the wavefunctions that include or exclude the $5\bar{d}$ and 5d DFAOs in the core of X, respectively.

3. RESULTS AND DISCUSSION

The results of the various relativistic and non-relativistic calculations of the molecular wavefunctions for the systems HgH^+, TlH, PbH^+ and BiH[1] are presented in this section.

In section 3.1, total molecular energies and dissociation energies predicted by these wavefunctions are analyzed and a chemical basis is determined for each system. For the chemical basis wavefunctions, the calculated expectation values of the dipole moment operator and virial ratios are given in section 3.2.

3.1 Chemical Basis Wavefunctions.

To simplify the discussion isoelectronic systems are treated together. The results of HgH^+ are presented and compared with the results reported for AuH [1]. Next, the results for TlH and PbH^+ are given, followed by the results for BiH.

For each system several wavefunctions are constructed. Based on an energetic criterion and on examination of the expansion coefficients of the valence RMOs of these wavefunctions, a chemical basis is determined consisting of those DFAOs having substantial participation in the formation of the molecule [1]. To visualize the participation of the various DFAOs in bonding, contour plots of a few representative RMOs are presented. Finally, in this section, plots of difference density for the 5d

---

[1]The non-relativistic results for BiH, are reported and compared with the relativistic results found by Malli and Pyper [32].

DFAOs, $\Delta\rho_{5d}$ defined in eq. 62, are given for the systems AuH, HgH^+, TlH, PbH^+ and BiH, to display the importance in bonding of these DFAOs through the series.

3.1.1 HgH^+ Molecular Wavefunctions

Eight molecular wavefunctions, four relativistic and their corresponding non-relativistic limits[2], were calculated for the experimental separation of 3.013 a.u. [33], using the following DFAO basis sets for the expansion of the valence RMOs:

B10 = {1s(H); $5\bar{d}$,5d,6s,$6\bar{p}$,6p (Hg^+)}[3],

B7 = {1s(H); $5\bar{d}$,5d,6s (Hg^+)},

B5 = {1s(H); 6s,$6\bar{p}$,6p (Hg^+)},

B2 = {1s(H); 6s (Hg^+)}, and for the NRMOs:

B10NR = {1s(H); 5d,6s,6p (Hg^+)},

B7NR = {1s(H); 5d,6s (Hg^+)},

B5NR = {1s(H); 6s,6p (Hg^+)} and

B2NR = {1s(H); 6s (Hg^+)},

where $\ell(\bar{\ell})$ is the DFAO with $j = \ell + 1/2$ ($j = \ell - 1/2$), and the notation Bn(BnNR), is used to specify a relativistic(non-relativistic) basis with n DFAOs of positive m.

The predicted molecular energies and dissociation energies given by these wavefunctions are reported in Table 1. For the

---

[2]All the non-relativistic (NR) wavefunctions were calculated by artificially increasing the velocity of light from c to 1000c.

[3]The DFAOs forming each basis are the only DFAOs allowed to form the valence wavefunction Φ_v (eq. 7). In each set, the 1s DFAO of hydrogen is one of the members and the others are DFAOs belonging to the heavy centre. The occupied DFAOs from the heavy centre not present in the basis are taken to form the core wavefunction Φ_c (eq. 6).

relativistic wavefunctions, the results show that when the 5d and 5d DFAOs are included in the basis (B10 or B7), there is an increase in the dissociation energy (De), compared with that predicted when the $5\bar{d}$ and 5d DFAOs are kept in the core (B5 or B2). This increase amounts to 0.380 eV or 0.429 eV, according to whether the $6\bar{p}$ and 6p DFAOs are present or absent in the basis. Both results are about 13% of the experimental De[4] of 3.11 eV [33] and although smaller, are comparable to the almost 1eV increase in De using similar bases in AuH [1]. As expected, the energy lowering in HgH^+ is smaller, because the $5\bar{d}$ and 5d DFAOs of Hg^+ are lower in energy than the hydrogen 1s DFAO by as much as half an atomic unit, whereas the $5\bar{d}$ and 5d DFAOs in the gold atom are nearly degenerate with the hydrogen 1s DFAO.

The contribution of the $6\bar{p}$ and 6p DFAOs to the dissociation energy is readily inferred from the 0.159 eV or 0.208 eV difference in the predicted De when using the bases B10 and B7 (which include the $5\bar{d}$ and 5d DFAOs) or the bases B5 and B2 (not including the $5\bar{d}$ and 5d DFAOs), respectively. These results are about 7% of the experimental De, indicating a non-negligible participation of the $6\bar{p}$ and 6p DFAOs in the bonding of HgH^+. The calculations on AuH [1] using similar basis sets, yielded about 3% of its experimental De. The greater participation of the $6\bar{p}$ and 6p DFAOs in HgH^+ is attributed to the fact that these DFAOs in Hg^+ are only 3 eV above the hydrogen 1s DFAO, as opposed to 10 eV in the gold atom.

---

[4] The experimental De value given includes the zero point energy of the molecule obtained from ref. [33]

TABLE 1. HgH^+ Total Energy E, and Dissociation Energy De, as predicted by various wavefunctions[a]. Non-relativistic results follow the Relativistic results.

Relativistic Basis	-(E+19653 a.u.)	De(eV[b])[c]
B10={1s;5$\bar{d}$,5d,6s,6$\bar{p}$,6p}	0.83134	0.657
B7 ={1s;5$\bar{d}$,5d,6s}	0.82548	0.498
B5 ={1s;6s,6$\bar{p}$,6p}	0.81736	0.277
B2 ={1s;6s}	0.80971	0.069
Non-relativistic(NR)	**-(E+18409 a.u.)**	**De(eV)**
B10NR={1s;5d,6s,6p}	0.23972	-0.061
B7NR ={1s;5d,6s}	0.23186	-0.275
B5NR ={1s;6s,6p}	0.23282	-0.248
B2NR ={1s;6s}	0.22468	-0.470

[a] Calculated for Re=3.011a.u.
[b] 1a.u.=27.21165eV
[c] De(exptl)=3.11eV, [33]

From this analysis of the predicted dissociation energies in HgH^+, it can be concluded that the chemical basis of HgH^+ should contain the 5$\bar{d}$, 5d, 6s,6$\bar{p}$ and 6p DFAOs from Hg^+ and the 1s DFAO of hydrogen as given by the basis B10 which predicts a De about 29% of the experimental value [33] and a total molecular energy of -19653.831 a.u.. On the other hand, the Dirac-Fock one-centre calculation of HgH^+ reported by Pyykko [8] predicted a total energy of -19653.678 a.u., using only 6s, 6$\bar{p}$ and 6p DFAOs in valence. This result is in better agreement with the total energy for HgH^+ of -19653.817 a.u., as predicted using the similar basis, B5, shown in Table 1.

For the non-relativistic wavefunctions, an important observation from Table 1 is their failure to predict any binding. Even the calculation for the valence wavefunction with

twelve electrons, B10NR, predicts an unbound HgH^+ system by 0.06 eV, whereas the corresponding relativistic wavefunction predicts it bound by 0.66 eV. Furthermore, analysing the relative increase obtained for the calculated dissociation energies, it is found that the inclusion of the 5d DFAOs in the basis yields an increase of 0.19 eV in De, while that of the 6p DFAOs gives an increase of 0.22 eV. This indicates a small and nearly equal participation of these DFAOs in bonding. In comparison with the relativistic results, the increase in De yielded by inclusion of the 6p DFAOs is similar. However, that of the 5d DFAOs is underestimated by 50%.

The above conclusions, similar to those reached for AuH [1], are further supported by examining the expansion coefficients of the occupied valence RMOs and NRMOs given in Table 2 for the chemical basis wavefunctions.

For the relativistic wavefunction, these coefficients indicate a significant mixing of the $5\bar{d}$ and 5d DFAOs of Hg^+ with the hydrogen 1s DFAO in the three valence RMOs $\phi_{\frac{1}{2},1}$, $\phi_{\frac{1}{2},2}$ and $\phi_{\frac{1}{2},3}$ with m=1/2. In contrast, only the $\phi^{NR}_{\frac{1}{2},1}$ and $\phi^{NR}_{\frac{1}{2},3}$ NRMOs with m=1/2, have substantial mixing of the 5d DFAOs with the 1s DFAO. The other NRMO, $\phi^{NR}_{\frac{1}{2},2}$, is a pure $5d_\pi$ orbital with $[\alpha>$-spin that is degenerate with the NRMO $\phi^{NR}_{\frac{3}{2},1}$ which is a $5d_\pi$ orbital with $[\beta>$-spin.

In comparison with the AuH RMOs [1], similar features are observed. For this reason, the amplitude of the first component of the lowest and highest occupied RMOs of AuH having

TABLE 2. SCF Relativistic and Non-relativistic Wavefunctions for HgH^+ at R(exptl)=3.013a.u. Computed by using the Chemical Basis.

BASIS	R M O s					
	$\phi_{\frac{1}{2},1}$[a]	$\phi_{\frac{1}{2},2}$	$\phi_{\frac{1}{2},3}$	$\phi_{\frac{3}{2},1}$	$\phi_{\frac{3}{2},2}$	$\phi_{\frac{5}{2},1}$
	-1.0179[b]	-0.9454	-0.7017	-0.9939	-0.9257	-0.9146
H:1s	0.1617	0.1763	-0.5119	-	-	-
Hg^+:5$\bar{d}$	-0.9536	0.2278	-0.1538	-0.9962	-0.0873	-
Hg^+:5d	0.1595	0.9369	0.2483	0.0873	-0.9962	1.0000
Hg^+:6s	0.0024	-0.0045	0.6045	-	-	-
Hg^+:6$\bar{p}$	-0.0013	0.0044	-0.0785	-	-	-
Hg^+:6p	0.0060	0.0030	0.0670	-0.0012	-0.0004	-

BASIS	N R M O s					
	$\phi^{NR}_{\frac{1}{2},1}$	$\phi^{NR}_{\frac{1}{2},2}$	$\phi^{NR}_{\frac{1}{2},3}$	$\phi^{NR}_{\frac{3}{2},1}$	$\phi^{NR}_{\frac{3}{2},2}$	$\phi^{NR}_{\frac{5}{2},1}$
	-1.0620	-1.0410	-0.6297	-1.0410	-1.0351	-1.0351
H:1s	0.1617	-0.0001	0.6269	-	-	-
Hg^+:5$\bar{d}$	-0.6088	-0.7747	0.1423	0.4470	0.8945	-
Hg^+:5d	0.7459	0.6323	-0.1744	-0.8945	0.4470	1.0000
Hg^+:6s	0.0221	-0.0000	-0.4830	-	-	-
Hg^+:6$\bar{p}$	-0.0118	-0.0042	0.0727	-	-	-
Hg^+:6p	0.0166	0.0030	-0.1028	-0.0052	-0.0000	-

[a] The first subscript denotes the R(NR)MOs m quantum numbers and the second subscript is just an index to differenciate between R(NR)MOs with same m.
[b] R(NR)MO eigenvalues in a.u.

m=1/2, $\phi_{\frac{1}{2},1}$ and $\phi_{\frac{1}{2},3}$ are plotted in figure 2. As can be seen for $\phi^{1}_{\frac{1}{2},1}$, the hydrogen $1s_\sigma$ orbital is in bonding phase to the $5d_\sigma$ gold orbital which has its positive lobes in the z-axis. Near the gold atom, the observed changes in the

amplitude sign simply reflect the nodal structure of the 5d radial part.

For $\phi^1_{\frac{1}{2},3}$, the hydrogen 1s orbital which is positive is in antibonding phase with the z-lobe of the $5d_\sigma$ (in HgH^+, the coefficients of $\phi^1_{\frac{1}{2},3}$ are reversed in sign), but it is in bonding phase with the perpendicular lobes of the $5d_\sigma$ that are positive and broader due to the significant contribution of the gold atom $6s_\sigma$ orbital. Apart from a sign, these plots are essentially the same as those reported by Krauss and coworkers [34], in their relativistic effective core potential calculation for AuH.

For a further investigation of the 5d-6s-6p hybridization in HgH^+, the localization procedure used by Malli and Pyper for AuH [1], with the criterion that the hydrogen 1s DFAO contributes only to one localized MO, was applied to the m=1/2 valence R(NR)MOs of the chemical basis. The form of the resulting localized orbitals clarifies the effective 5d-6s-6p hybridization on HgH^+ and gives a simpler description of the chemical bond in HgH^+ in terms of only one bonding orbital, as would be expected for the interaction of Hg^+ with one electron in hydrogen. The results are given in Table 3 and show that the localized R(NR)MOs [loc1> and [loc2> are non-bonding orbitals (with no participation of the hydrogen 1s) concentrating electron density off the internuclear axis, whereas the other one [loc3>, concentrates charge along it and is the bonding orbital.

Figure 2. RMO plots for AuH.

Amplitude orbital plots of the first component of the valence RMOs $\Phi_{\frac{1}{2},1}$ and $\Phi_{\frac{1}{2},3}$ (m = 1/2) of the chemical basis wavefunction for AuH [1], at an internuclear distance of 2.8794 a.u. The outermost contour is fixed at 0.0884 a.u. and the ratio between successive inner contours is 2.
Solid or dashed lines are positive or negative contours, respectively.

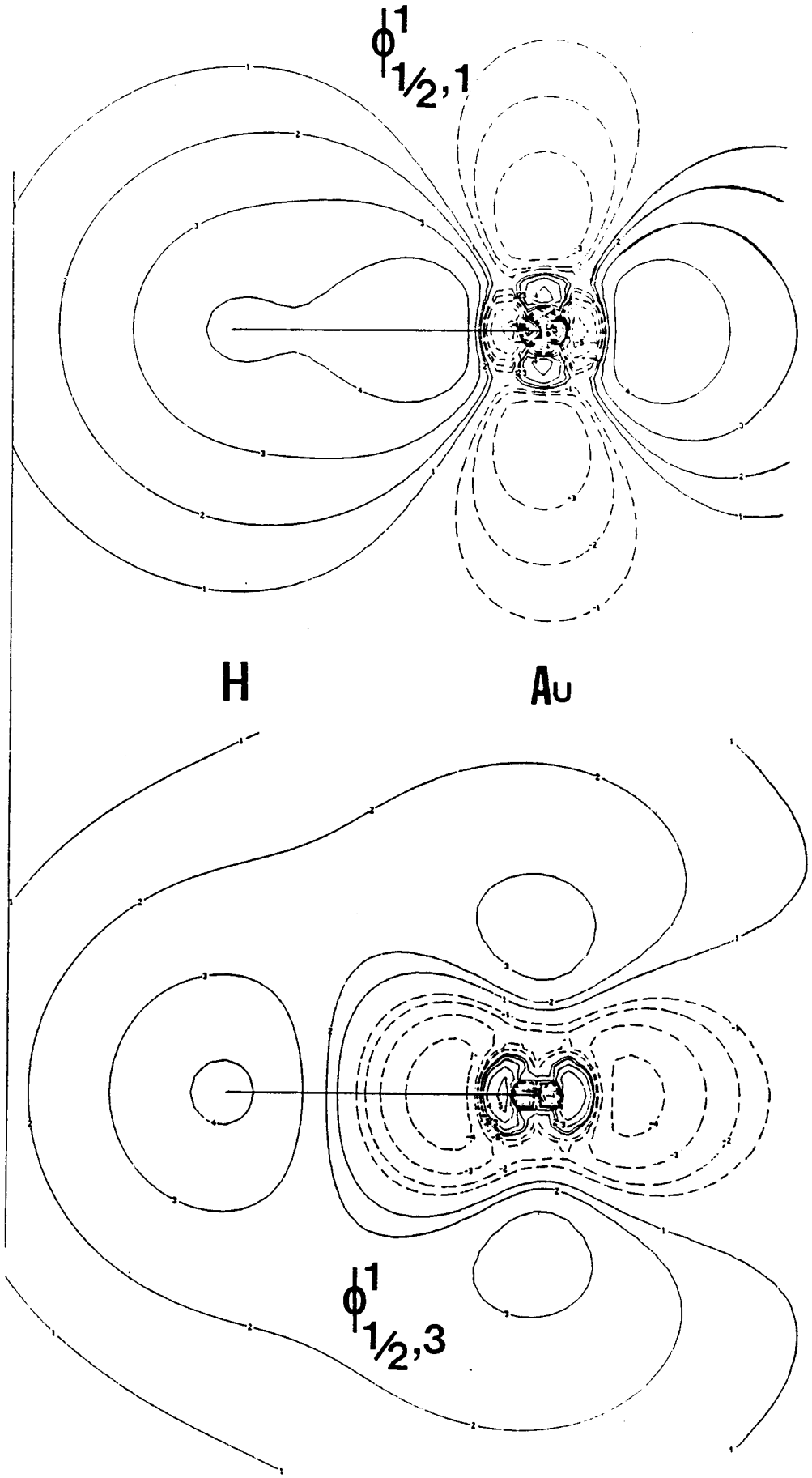
$\phi^1_{1/2,1}$
H
Au
$\phi^1_{1/2,3}$

TABLE 3. HgH^+ Chemical Basis Set Localized Molecular Orbitals of m=1/2.

Basis	Localized RMOs			Localized NRMOs		
	[loc1>	[loc2>	[loc3>	[loc1>	[loc2>	[loc3>
H:1s	0.00	0.00	0.565	0.00	0.00	0.647
Hg^+:5$\bar{d}$	-0.857	0.497	-0.062	0.775	-0.625	-0.014
Hg^+:5d	-0.516	-0.828	0.113	0.632	0.766	0.017
Hg^+:6s	0.005	-0.254	-0.548	0.00	0.142	-0.462
Hg^+:6$\bar{p}$	-0.004	0.031	0.072	0.004	-0.030	0.067
Hg^+:6p	0.002	-0.034	-0.058	0.003	0.042	-0.095

Both relativistic and non-relativistic wavefunctions have similar characteristics for [loc1> and [loc2>. However, there is a striking difference for the predicted 5d-6s hybridization in the [loc3> bonding NRMO, which fails to predict the substantial contribution given by the 5$\bar{d}$ and 5d DFAOs to the [loc3> bonding RMO. Therefore, the proposed hybridization of (n-1)dns given by Orgel [37] to explain the two-coordination of Hg in linear systems can be understood for a relativistic wavefunction only. Furthermore, the polarity of HgH^+ molecule is overestimated by the non-relativistic wavefunction, as judged by the increased contribution of the hydrogen 1s DFAO to the bonding orbital [loc3> compared with the relativistic case.

3.1.2 TlH and PbH^+ Molecular Wavefunctions

For each molecule, six molecular wavefunctions (three relativistic and the corresponding three non-relativistic limits) were calculated using the following DFAO basis sets for the expansion of the valence RMOs :

B10 = {1s(H); $5\bar{d}$,5d,6s,$6\bar{p}$,6p (Tl of Pb^+)},

B5 = {1s(H); 6s,$6\bar{p}$,6p (Tl or Pb^+)},

B4 = {1s(H); $6\bar{p}$,6p (Tl or Pb^+)} and the valence NRMOs:

B10NR= {1s(H); 5d,6s,6p (Tl or Pb^+)},

B5NR = {1s(H); 6s,6p (Tl or Pb^+)} and

B4NR = {1s(H); 6p (Tl or Pb^+)}.

These basis sets were chosen to investigate the contribution of the $5\bar{d}$, 5d and 6s DFAOs of Tl and Pb^+ to the bonding in TlH and PbH^+ respectively.

For TlH, the wavefunctions were calculated at the experimental distance of 3.534 a.u. [33]. Unfortunately, for PbH^+ there is no experimental bond length. Therefore, an equilibrium distance was obtained by fitting a polynomial to four computed values of the molecular energy, using the basis B5 for the internuclear separations of 3.250 a.u., 3.450 a.u., 3.550 a.u. and 3.650 a.u.. The best fit gave 3.5884 a.u. for the equilibrium distance. All the other wavefunctions of PbH^+ were calculated for 3.5884 a.u..

The predicted molecular energies and dissociation energies given by the various wavefunctions are given in Tables 4 and 5, for TlH and PbH^+, respectively.

For TlH, the increase in the calculated De when the $5\bar{d}$ and 5d DFAOs are included to enlarge the B5 basis (see Table 4) is 0.060 eV and 0.041 eV for the relativistic and non-relativistic wavefunctions, respectively. These results represent only about 3% of the experimental De of 2.06 eV [33], indicating an insignificant role of the $5\bar{d}$ and 5d DFAOs of Tl in the bonding of TlH. However, the role of the 6s DFAO of Tl is more important, as judged from the increase in De of 0.416 eV or 0.600 eV between the predictions of B5 or B5NR and that of the wavefunctions B4 or B4NR, respectively. These results represent 20% or 29% of the experimental De, for the relativistic and non-relativistic cases, respectively.

From the above calculations it is clear that the non-relativistic wavefunctions predict similar results for the importance of the 5d and 6s DFAOs of Tl in the bonding of TlH. However, there is a marked difference between the predicted dissociation energies for the non-relativistic and relativistic wavefunctions. For example, the non-relativistic De predicted for the wavefunction B5NR is 0.61 eV larger than that predicted for the relativistic wavefunction B5.

Pitzer [10], has pointed out that since the single valence electron in the thallium atom occupying a $6\bar{p}$ DFAO is $(1/3)\sigma$ bonding and $(2/3)\pi$ antibonding, the $6p_\sigma$ combination

TABLE 4. TlH Total Energy E, and Dissociation Energy De, as predicted by various wavefunctions[a]. Non-relativistic results follow the Relativistic Results.

Relativistic Basis	-(E + 20280 a.u.)	De(eV[b])[c]
B10={1s;5$\bar{d}$,5d,6s,6$\bar{p}$,6p}	0.66299	0.722
B5 ={1s;6s,6$\bar{p}$,6p}	0.66081	0.662
B4 ={1s;6$\bar{p}$,6p}	0.64585	0.246
Non-Relativistic Basis	**-(E + 18962 a.u.)**	**De(eV)**
B10NR={1s;5d,6s,6p}	0.37491	1.315
B5NR ={1s;6s,6p}	0.37340	1.274
B4NR ={1s;6p}	0.35135	0.674

[a] Calculated for Re(exptl)=3.534 a.u. [33]
[b] 1 a.u.=27.21165 eV
[c] De(exptl)=2.06 eV [33]

TABLE 5. PbH^+ Total Energy E, and Dissociation Energy De, as predicted by various wavefunctions[a].Non-Relativistic Results follow the Relativistic Results.

Relativistic Basis	-(E + 20919 a.u.)	De(eV[b])
B10={1s;5$\bar{d}$,5d,6s,6$\bar{p}$,6p}	0.89956	0.231
B5 ={1s;6s,6$\bar{p}$,6p}	0.89858	0.205
B4 ={1s;6$\bar{p}$,6p}	0.88834	-0.072
Non-Relativistic Basis	**-(E + 18962 a.u.)**	**De(eV)**
B10NR={1s;5d,6s,6p}	0.30949	1.213
B5NR ={1s;6s,6p}	0.30885	1.195
B4NR ={1s;6p}	0.29447	0.804

[a] Calculated for Re=3.588 a.u.
[b] 1 a.u.=27.21165 eV

$\sqrt{1/3}(6\bar{p}) \pm \sqrt{2/3}(6p)$ is needed to form a σ-bond with the hydrogen 1s DFAO. For the relativistic calculation, this requires 0.63 eV of promotion energy, corresponding to 2/3 of the calculated splitting between the $6\bar{p}$ DFAO and the unoccupied 6p DFAO, whereas no promotion energy is required for the non-relativistic case, since both $6\bar{p}$ and 6p DFAOs are degenerate.

From Table 5 it is clear that similar results are obtained for PbH^+. For the relativistic wavefunctions there is an increase of 0.277 eV when, in addition to the $6\bar{p}$ and 6p DFAOs, the 6s DFAO of Pb^+ is included in the basis. This increase is only 0.021 eV more, if the $5\bar{d}$ and 5d DFAOs are also included.

For the PbH^+ non-relativistic limit wavefunctions the corresponding contribution of 6s DFAO and 5d DFAOs to De are 0.391 eV and 0.031 eV, respectively.

Moreover, larger non-relativistic predictions for De are also found in PbH^+, viz. the non-relativistic wavefunction B5NR predicts a De that is 0.99 eV larger than that of the relativistic wavefunction B5. This can also be explained in terms of the promotion energy, because 2/3 of the calculated splitting between the $6\bar{p}$ and 6p DFAOs in Pb^+ amounts to 1.17 eV.

It can be concluded from the above results that the chemical basis for TlH and PbH^+, should include the 6s, $6\bar{p}$ and 6p DFAOs in addition to the hydrogen 1s DFAO. This basis predicts for TlH a total molecular energy of -20280.661 a.u. and a dissociation energy of 0.662 eV (32% of De(exptl)). In contrast, the

TABLE 6. SCF Relativistic and Non-relativistic Wavefunctions for TlH at R(exptl)=3.534 a.u. Computed by using the Chemical Basis.

BASIS	R M O s		N R M O s	
	$\phi_{\frac{1}{2},1}$[a]	$\phi_{\frac{1}{2},2}$	$\phi_{\frac{1}{2},1}$	$\phi_{\frac{1}{2},2}$
	-0.5153[b]	-0.2961	-0.4656	-0.2720
H:1s	0.3843	-0.5759	0.5415	-0.4711
Tl:6s	-0.7792	-0.5835	-0.6026	-0.7414
Tl:6$\bar{p}$	0.0465	-0.4053	0.0753	-0.2926
Tl:6p	-0.0436	0.3287	-0.1065	0.4139

[a] See Table 2.
[b] MO eigenvalues in a.u.

TABLE 7. SCF Relativistic and Non-relativistic Wavefunctions for PbH^+ at R=3.5884 a.u. Computed by using the Chemical Basis.

BASIS	R M O s		N R M O s	
	$\phi_{\frac{1}{2},1}$[a]	$\phi_{\frac{1}{2},2}$	$\phi_{\frac{1}{2},1}$	$\phi_{\frac{1}{2},2}$
	-0.8692[b]	-0.5952	-0.7790	-0.5684
H:1s	0.2542	-0.5848	0.3960	-0.5299
Pb^+:6s	-0.8813	-0.4387	-0.7556	-0.6158
Pb^+:6$\bar{p}$	0.0354	-0.4838	0.0680	-0.3100
Pb^+:6p	-0.0387	0.3096	-0.0962	0.4384

[a] See Table 2.
[b] MO eigenvalues in a.u.

Dirac-Fock one-centre calculation for TlH [7] predicts a total energy of -20280.374 a.u. using a basis with only the 6$\bar{p}$ and 6p DFAOs, which yields an unbound molecule of TlH by 7.1eV.

The coefficients of expansion of the valence RMOs for the chemical basis of TlH and PbH^+ are given in Tables 6 and 7, respectively. As can be noted, the valence RMOs of TlH and PbH^+ have similar features. In both cases the RMO $\phi_{\frac{1}{2},1}$ is a bonding orbital formed mostly by the 6s DFAO and the 1s DFAO of hydrogen, but with mixing coefficients reflecting the fact that the relative energy difference between the 1s DFAO of hydrogen and the 6s DFAO of Pb^+ is larger than that of the 6s DFAO of Tl in the isolated atoms.

The other RMO, $\phi_{\frac{1}{2},2}$, which is the HOMO, shows significant 6s-6p hybridization such that the hydrogen 1s DFAO is in antibonding phase with the 6s DFAO and in bonding phase with the $6\bar{p}$ and 6p DFAOs. By analysing only the large components of the HOMO of TlH, it is found that the [α>-spin component $\phi^1_{\frac{1}{2},2}$, is the combination $-0.58(1s_\sigma H)-0.78(6s_\sigma Tl)+0.50(6p_\sigma Tl)$ and the [β>-spin component $\phi^2_{\frac{1}{2},2}$, is $-0.14(6p_\pi Tl)$, which shows the character of the spin-orbit mixing as a small π-nonbonding orbital centered on thallium. Similarly, in PbH^+ the π-nonbonding orbital-component is $-0.22(6p_\pi Pb^+)$, and has a larger coefficient due to the larger splitting of the $6\bar{p}$ and 6p DFAOs in Pb^+ than in Tl. The two components of the HOMO $\phi_{\frac{1}{2},2}$ of TlH are plotted in figure 3.

In contrast, none of the valence NRMOs has any π-character because, as can be noted from Table 6 and 7, the coefficients for the $6\bar{p}$ and 6p DFAOs are in the ratio $-1:\sqrt{2}$, respectively, which yields a $6p_\sigma$ orbital with [α>-spin.

Figure 3. RMO plots for TlH.

Amplitude orbital plots of the first and second components, $\phi^{1}_{\frac{1}{2},2}$ and $\phi^{2}_{\frac{1}{2},2}$, of the HOMO of the chemical basis wavefunction for TlH at an internuclear separation of 3.534 a.u. The outermost contour is fixed at 0.0112 a.u. and the ratio between successive inner contours is $(1.9)^2$.
Solid or dashed lines are positive or negative contours, respectively.

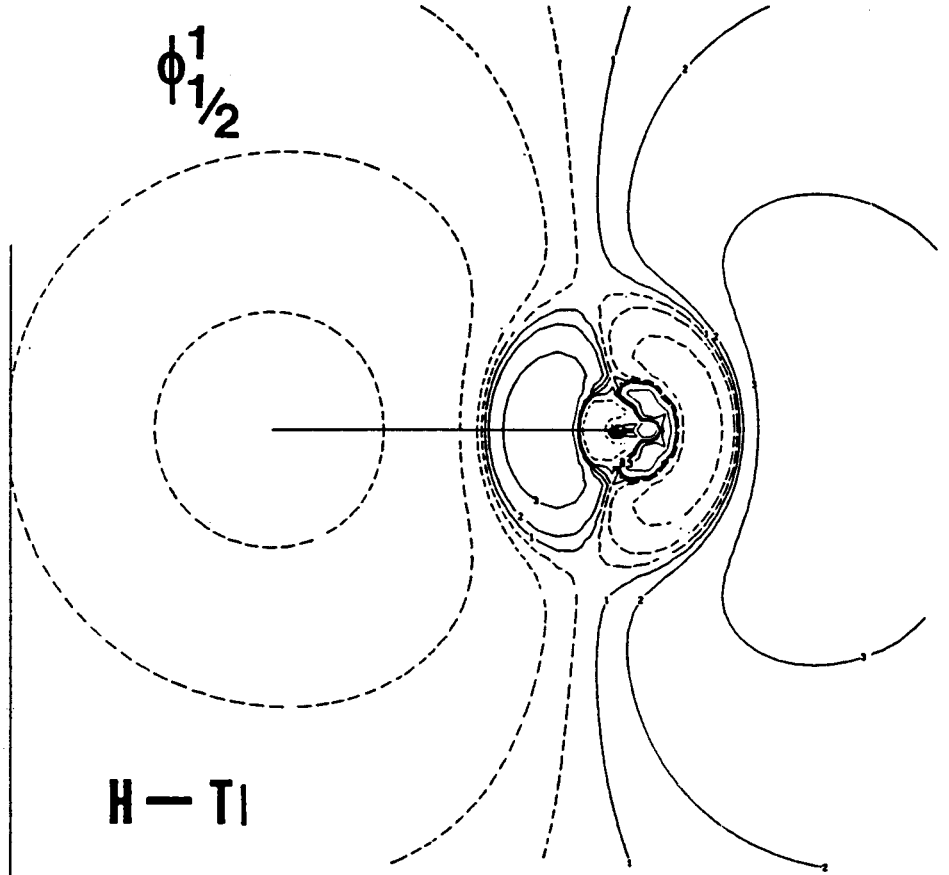
$\phi^1_{1/2}$
H — Tl

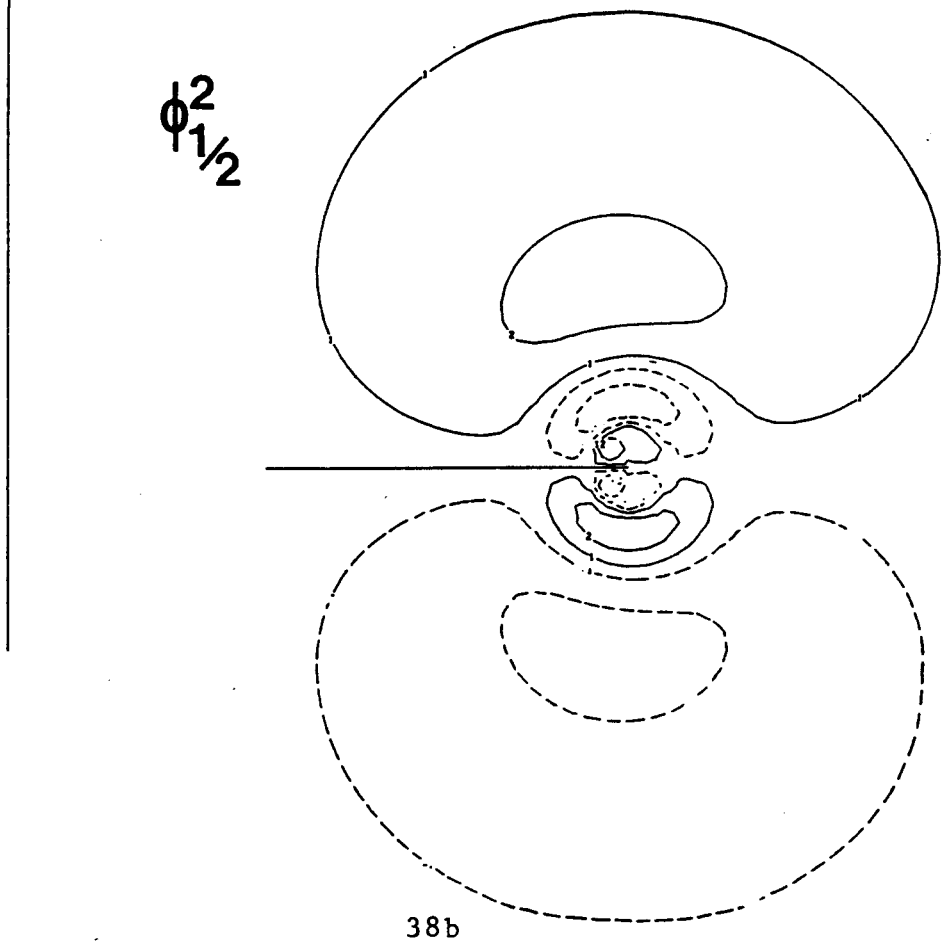
$\phi^2_{1/2}$

3.1.3 BiH Molecular Wavefunctions

Using similar DFAO basis sets as those used in TlH and PbH^+ for the expansion of the valence RMOs, Malli and Pyper [32] found that the chemical basis of BiH should consist of the 6s, $6\bar{p}$ and 6p DFAOs of bismuth and the 1s DFAO of hydrogen. In this section the corresponding non-relativistic limit ($c \rightarrow 1000c$) wavefuntions are reported.

These wavefunctions were calculated for the experimental internuclear separation of 3.411 a.u. Their predicted molecular energies and dissociation energies are given in Table 8, which also includes the relativistic results [32]. As can be seen from this table, the relativistic and non-relativistic wavefunctions predict a similar dissociation energy increase on enlarging the basis that contains the $6\bar{p}$ and 6p DFAOs of bismuth. When the 6s DFAO of Bi is included, this increase yields 0.228 eV for the relativistic case and 0.359 eV for the non-relativistic case and when the $5\bar{d}$ and 5d DFAOs also enter the basis, there is a similar increase of 0.259 eV and 0.376 eV, respectively.

This justifies the use of only the 6s, $6\bar{p}$ and 6p DFAOs of bismuth in the chemical basis. However, the noticeable difference between the relativistic and non-relativistic wavefunctions is that the latter fail to predict a bound molecule of BiH. By using the chemical basis, BiH is predicted to be bound by 0.428 eV in the relativistic case, which is about 14% of the experimental De of 3.00 eV [33], while it is predicted to be unbound by 0.305 eV in the non-relativistic

TABLE 8. BiH Total Energy E, and Dissociation Energy De, as predicted by various wavefunctions[a] Non-relativistic results follow the Relativistic[b] results.

Relativistic Basis	-(E+21572 a.u.)	De(eV[c])[d]
B10={1s;5$\bar{d}$,5d,6s,6$\bar{p}$,6p}	0.79824	0.459
B5 ={1s;6s,6$\bar{p}$,6p}	0.79711	0.428
B4 ={1s;6$\bar{p}$,6p}	0.78873	0.200
B4(1c)[e]={1s;6$\bar{p}$,6p}	0.78744	0.622
B3(1c)={1s;6p}	0.76100	-0.099
Non-relativistic(NR) Basis	**-(E+20096 a.u.)**	**De(eV)**
B10NR={1s;5d,6s,6p}	0.07709	-0.288
B5NR ={1s;6s,6p}	0.07644	-0.305
B4NR ={1s;6p}	0.06328	-0.664

[a] Calculated for Re(exptl)=3.411 a.u. [33]
[b] The results for B10, B5 and B4 are from ref.[16]
[c] 1 a.u.=27.21165 eV
[d] De(exptl)=3.00 eV [33]
[e] Basis B4(1c) and B3(1c) were constructed using a one configuration wavefunction for Bi and differ from all the other calculations that used a 5-configuration wavefunction for Bi.

case.

The energy shift of the non-relativistic De predictions with respect to the relativistic ones is almost the same and is about 0.78 eV on the average. For this reason two more calculations were performed to investigate the importance of the 6$\bar{p}$ DFAO in the relativistic case, because there is already 2.1 eV difference in energy for this DFAO with respect to the 6p DFAO in the bismuth atom. The basis sets for these calculations were:

B4(1c)={1S(H),6$\bar{p}$,6p(Bi)}

and

B3(1c)={1s(H),6p(Bi)},

TABLE 9. SCF Relativistic[a] and Non-relativistic Wavefunctions for BiH at R(exptl)=3.411 a.u. Computed by using the Chemical Basis.

Basis	R M O s			N R M O s		
	$\phi_{\frac{1}{2},1}$[b]	$\phi_{\frac{1}{2},2}$	$\phi_{\frac{1}{2},3}$	$\phi^{NR}_{\frac{1}{2},1}$	$\phi^{NR}_{\frac{1}{2},2}$	$\phi^{NR}_{\frac{1}{2},3}$
	-0.7235[c]	-0.4090	-0.3033	-0.6390	-0.4009	-0.2940
H:1s	0.2241	-0.5624	0.2860	-0.3670	0.5595	0.0001
Bi:6s	-0.8968	-0.3982	0.1585	0.7782	0.5958	0.0000
Bi:6$\bar{p}$	0.0301	-0.5599	-0.7338	-0.0547	0.3055	-0.8165
Bi:6p	-0.0166	-0.2581	-0.5994	0.0774	-0.4320	-0.5773

[a] From Reference [16]
[b] See Table 2.
[c] R(NR)MO eigenvalues in a.u.

where 1c indicates that the wavefunction of bismuth was constructed from one configuration only, namely the one having 2 electrons occupying the 6$\bar{p}$ DFAO and 1 electron in the 6p DFAO, and is to be distinguished from the previous calculations where the bismuth wavefunction was built from five configurations.

The difference in the predicted dissociation energy for B4 and B4(1c) is 0.42 eV, and this is just the 0.46 eV that the total bismuth atomic energy predicted by the one-configuration wavefunction is above that predicted by the five-configuration wavefunction. However, from the predicted energy difference between B4(1c) and B3(1c), which is about 0.72 eV, it can be concluded that the energy difference in De predicted for the relativistic and non-relativistic wavefunctions is, in part, due to the removal of the degeneracy of the three 6p electrons of the bismuth atom.

The coefficients of expansion of the valence RMOs and NRMOs of the chemical basis wavefunctions B4 and B4NR are reported in Table 9. Clearly, the first molecular orbital $\phi_{\frac{1}{2},1}$ or $\phi^{NR}_{\frac{1}{2},1}$, is a bonding orbital of the 6s DFAO of bismuth and the 1s DFAO of hydrogen. The second one $\phi_{\frac{1}{2},2}$ or $\phi^{NR}_{\frac{1}{2},2}$, which is higher in energy, is the antibonding combination of the 6s and the 1s DFAOs, but is bonding for the σ-part of the $6\bar{p}$ and 6p DFAOs of bismuth with the 1s DFAO of hydrogen.

The highest occupied orbital, however, shows a marked difference in form for the relativistic and non-relativistic wavefunctions. The NRMO, viz. $\phi^{NR}_{\frac{1}{2},3}$, is a pure $6p_{\pi}$ nonbonding orbital with $[\beta>$-spin, whereas the $\phi_{\frac{1}{2},3}$ RMO is only 90% in π-character and has a spin-orbit mixing component with $[\alpha>$-spin as an antibonding combination of the hydrogen 1s DFAO and the 6s DFAO of bismuth. The two components of the RMO $\phi_{\frac{1}{2},3}$ are plotted in figure 4 to illustrate these features.

3.1.4 $\Delta\rho_{5d}$ Contour Plots.

Difference density plots $\Delta\rho_{5d}$ (eq. 62) highlighting the importance in bonding of the 5d and 5d DFAOs were generated for the relativistic wavefunctions of AuH, HgH^+, TlH, PbH^+ and BiH and are shown in figure 5. For each plot the outermost positive contour line (solid) is fixed at 0.02 a.u. and the succesive inner lines increase in value by a factor of 2 to a maximum value of 0.32 a.u..

Figure 4. RMO plots for BiH.

Amplitude orbital plots of the first and second components, $\phi^{1}_{\frac{1}{2},3}$ and $\phi^{2}_{\frac{1}{2},3}$, of the highest occupied RMO of the chemical basis wavefunction for BiH at an internuclear separation of 3.411 a.u. The outermost contour is fixed at 0.02 a.u. and the ratio between succesive inner contours is 2.
Solid or dashed lines are positive or negative contours, respectively.

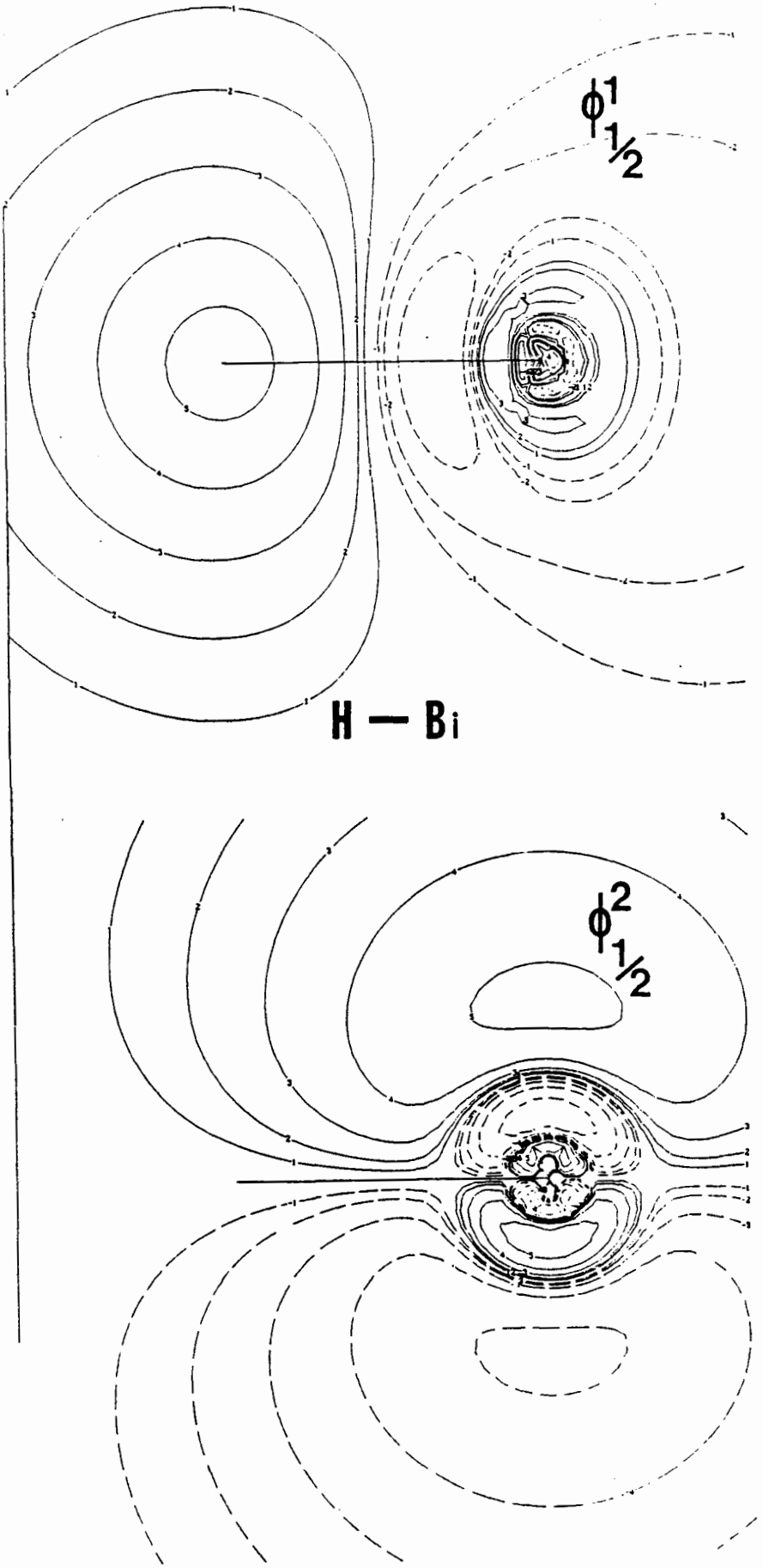
$\phi^1_{1/2}$
H — Bi
$\phi^2_{1/2}$

The more pronounced 5d charge density redistribution is for AuH and HgH^+ in comparison with that for TlH, PbH^+ or BiH, as jugded by the number and size of the contour lines shown. Specifically, the form of the positive contour lines in AuH or HgH^+ indicates that near the heavy center, part of a d_σ-type density has been shifted to outer regions, off the internuclear axis and near the hydrogen atom, which is shown by the negative contours. However, for the systems TlH, PbH^+ and BiH, the plots show that the off-axis lobes of the d_σ-type density have disappeared. Furthermore, the charge redistributions for these three systems are minute and only located on the heavy nuclear charge and not on the H, which indicates that there is no significant mixing between the 1s DFAO of hydrogen and the $5\bar{d}$ and 5d DFAOs of the heavy centre.

These plots pictorially confirm that the $5\bar{d}$ and 5d DFAOs are important in the bonding of AuH or HgH^+, but they cease participating in the bonding of TlH, PbH^+ or BiH.

Figure 5. $\Delta\rho_{5d}$ Difference density contour plots for AuH, HgH^+, TlH, PbH^+ and BiH.

$\Delta\rho_{5d} = \rho' - \rho''$, where ρ' is the total charge density when the $5\bar{d}$ and 5d DFAOs of the heavy centre are part of the core, and ρ'' is the charge density when they are part of the valence.
The outermost contour is fixed at 0.02 a.u. and successive inner contours increase in a ratio of 2. Solid or dashed lines are positive or negative contours, respectively.

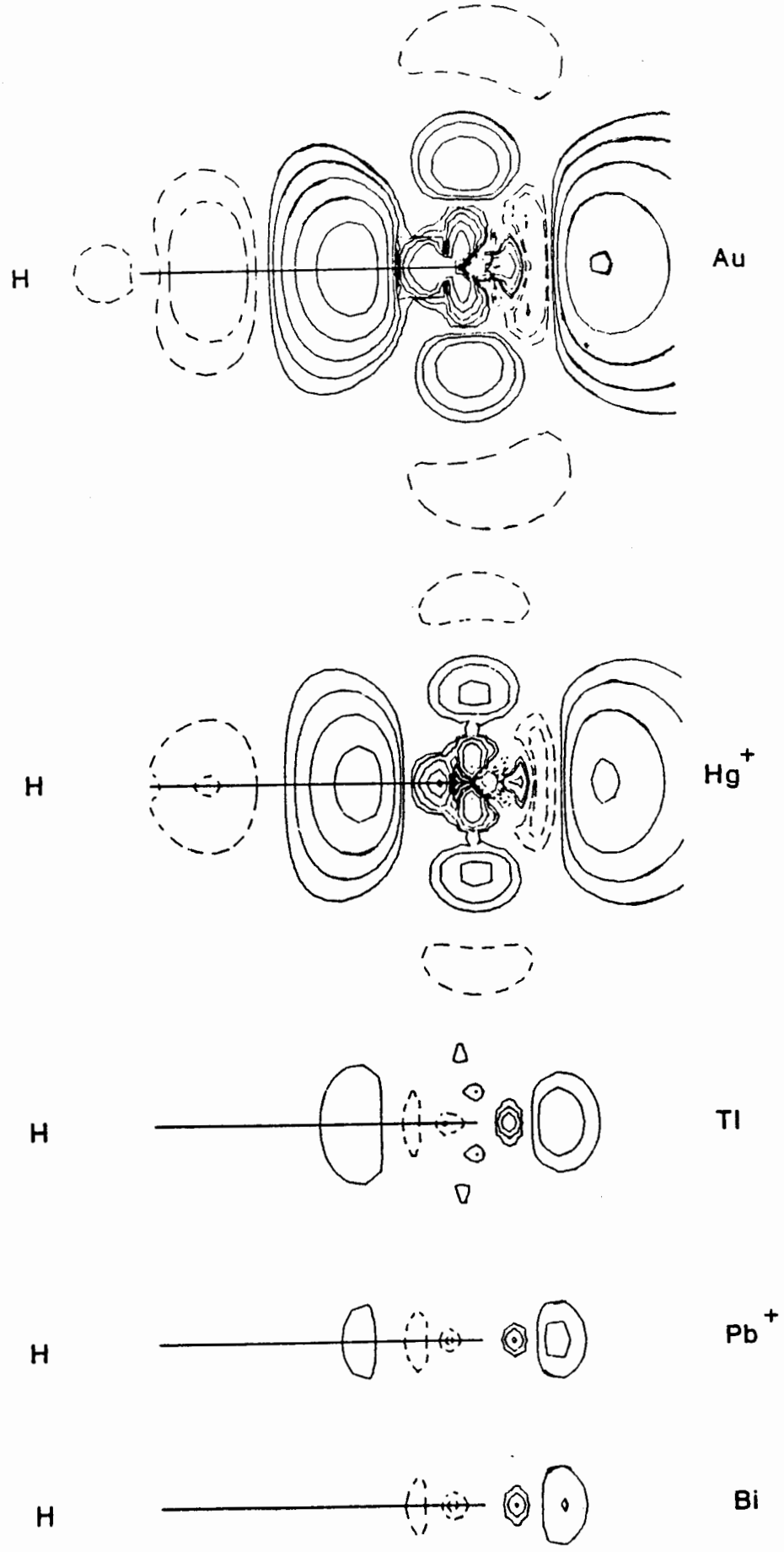
H
Au
H
Hg+
H
Tl
H
Pb+
H
Bi

3.2 Dipole Moments and Virial Ratios.

In this subsection the dipole moment results of the systems under study are presented. For testing the dipole moment programme, the total dipole moment of LiH was calculated and is given in the test cases part. Next, the dipole moment calculations of AuH using the various accuracy wavefunctions reported by Malli and Pyper [1] are given. Finally, the dipole moments and virial ratios of the systems HgH^+, TlH, PbH^+ and BiH are calculated using the chemical basis wavefunctions reported in section 3.1.

3.2.1 Test Cases.

For testing the one-centre and two-centre atomic dipole moment integrals, a series of calculations were performed using an atomic basis consisting of s, p and d-type Gaussian functions centered on H and on He at an internuclear separation of 2 a.u. Some of the results are given in Table 10 and are compared with the results produced by the HONDO programme with the same basis. As can be seen, the calculated values of these atomic dipole moment integrals are almost identical.

To test for the molecular dipole integrals and the total dipole moment evaluation, the LiH wavefunction reported by Cade and Huo [35] was used. The Slater functions forming the basis set of this wavefunction were transformed into numerical tabulated functions to be processed by the numerical integration routines of the programme. A total dipole of 2.3613 a.u. was

TABLE 10. One-centre and Two-centre Atomic Dipole Moment Integrals for HeH.

	Present Programme	H O N D O
One-Centre		
$\langle s\ (H)\ [z] p_\sigma\ (H)\rangle$	0.50000000[a]	0.50000000
$\langle p_\sigma (H)\ [z] d_\sigma\ (H)\rangle$	0.57735027	0.57735027
$\langle p_\pi (H)\ [z] d_\pi\ (H)\rangle$	0.50000000	0.50000000
$\langle s\ (He)[z] p_\sigma (He)\rangle$	0.35355339	0.35355339
$\langle p_\sigma (He)[Z] d_\sigma (He)\rangle$	0.40824829	0.40824829
$\langle p_\pi (He)[Z] d_\pi (He)\rangle$	0.35355339	0.35355339
Two-Centre		
$\langle s\ (H)[z] p_\sigma (He)\rangle$	-0.00999514	-0.00999515
$\langle p_\sigma (H)[z] d_\sigma (He)\rangle$	-0.02538982	-0.02538981
$\langle p_\pi (H)[z] p_\pi (He)\rangle$	0.01999031	0.01999031
$\langle p_\pi (H)[z] d_\pi (He)\rangle$	-0.00942352	-0.00942352
$\langle d_\delta (H)[z] d_\delta (He)\rangle$	0.01884704	0.01884704

[a] Values are in a.u. and refer to a coordinate system centered at the midpoint between He and H and with positive z-axis pointing towards H.

found in comparison with 2.3614 a.u. of Cade and Huo [35]. This result proves again the well functioning of the programme, because the small difference of 0.0001 a.u. between the two values can be attributed to the truncation errors incurred in the numerical integrations.

To test the correct calculation of a molecular dipole integral with symmetry other than σ, the π-type molecular dipole integral for CO was calculated using the π-type molecular orbital of the CO wavefunction of Huo [36]. In agreement with Huo's result, a value of -2.2888 a.u. was found for this integral.

Unfortunately, for the systems under study (AuH, HgH^+, TlH, PbH and BiH) no experimental dipole moment values are known. Therefore, as a test of the validity of using wavefunctions of chemical basis level to calculate their dipole moments, the dipole moments of some systems with known experimental values were calculated. The dipole moments for TlI and PbTe were evaluated by using the chemical basis functions calculated by Malli [38].

In addition, the dipole moment of LiH was calculated by using the chemical and the extended (including polarization functions) basis wavefunctions reported by Malli and Pyper [1].

The results are shown in Table 11 and comparison with their experimental values indicates a better than qualitative agreement. For LiH, for example, the chemical basis has a relative error of 11% with respect to the experimental value of 2.3142 a.u. [33], whereas the extended basis has a relative error of only 2%. For TlI, a very good agreement with the experimental value is found with a relative error of 5%, and for PbTe the relative error is 19%.

3.2.2 AuH Dipole Moment Calculation.

Dipole moment calculations were performed using the gold hydride wavefunctions of varying basis size calculated by Malli and Pyper [1]. The results of these calculations are shown in Table 12. The predicted dipole moment curves for the two extended basis wavefunctions EB27 (chemical basis plus

TABLE 11. Dipole Moments for LiH, TlI and PbTe calculated by using Chemical Basis Wavefunctions.

A-B[a]	μ(a.u.[b])	EXP[c]
LiH	2.5753 (2.3668[d])	2.3141
TlI	1.9078	1.8137
PbTe	1.2655	1.0623

[a] All values indicate A^+B^- polarity.
[b] 1 a.u.=2.54177 D
[c] Experimental values from reference [33]
[d] Using extended basis functions from reference [1].

TABLE 12. AuH Dipole Moment Curves.[a]

	μ(a.u.[b])				
R(a.u.)	CB	EB20	ECP[c]	EB27	RCI
2.6294	0.968[d]	0.905	-	0.829	0.738
2.7500	-	-	0.957	-	-
2.8794[e]	0.976	0.984	-	0.901	0.802
3.0000	-	-	1.044	-	-
3.1294	0.967	1.046	-	0.956	0.846
3.2500	-	-	1.127	-	-
3.3794	0.968	1.132	-	1.045	0.909

[a] Calculated by using the wavefunctions from reference [1]; Chemical Basis (CB), extended basis with 20 basis (EB20) not including 5f polarization orbitals, extended basis including 5f polarization orbitals (EB27) and relativistic configuration interaction (RCI) wavefunction.
[b] 1 a.u.=2.54177 D.
[c] Effective core potential (ECP) results for the AREP wavefunction [34].
[d] All values indicate Au^+H^- polarity.
[e] Experimental Re [33].

polarization functions up to 5f' orbitals [1]) and EB20 (not including 5f' orbitals), and the relativistic configuration

interaction (RCI) wavefunction (obtained by including all the derived single and double excitations from the ground state EB27 SCF wavefunction [1]) show the same trend of increasing dipole moment upon increasing the AuH internuclear separation. These results are very similar to the ECP-ARREP calculations [34] also reported in Table 12. On the other hand, for the chemical basis (CB) wavefunction the predicted dipole moment values remain nearly constant upon increase of the distance R, which simply shows that the CB wavefunction is too poor to describe a smoothly varying curve for the dipole moment. However, it should be noted that for the experimental R=2.8794, the CB wavefunction predicted dipole moment value is 22% off the corresponding RCI value and only 8% of the corresponding EB27 value.

The non-relativistic dipole moment values for the CB, EB20 and EB27 non-relativistic limit wavefunctions, predicted at the experimental separation R=2.8794 a.u. [33], are reported and compared with the corresponding relativistic values in table 13.

The results show that the non-relativistic dipole moment values are larger in magnitude than the relativistic values. For example, for the EB27 wavefunction the non-relativistic predicted dipole moment is 50% larger than the corresponding relativistic dipole moment value of 0.901 a.u. These results confirm the prediction of a more polar AuH molecule in the non-relativistic case than in the relativistic one, as judged by comparing the 1s hydrogen orbital participation in the relativistic localized bonding orbital of the CB wavefunction

TABLE 13. AuH Non-Relativistic and Relativistic Dipole Moment and Energy Sensitivity. Calculated at Re(exptl)=2.8794a.u.

Basis	μ(a.u.)		E^a(eV)	
	NRel	Rel	NRel	Rel
CB[b]	1.373	0.976	0.00	0.00
EB20	1.434	0.984	0.49	0.60
EB27	1.363	0.901	0.54	0.66
CB+6pSL[c]	1.443	1.065	0.15	0.18
CB+6pDF[d]	1.925	1.271	0.19	0.10

[a] Energy lowering in eV with respect to the predicted total energy for the CB wavefunction.
[b] Chemical Basis CB consisting of $5\bar{d}$, 5d and 6s DFAOs of gold and the hydrogen 1s DFAO [1].
[c] CB plus 6p Slater type function with an exponent ζ=2.75 centered on gold.
[d] CB plus 6p DFAO as obtained from the MCDF calculation for the gold atom [1].

and its non-relativistic limit [1].

Furthermore, the less polar Au^+H^- relativistic prediction is also in agreement with the Mulliken population analyses of the relativistic and non-relativistic ECP wavefunctions of Hay et al. [11]. Again, it is interesting to note (see Table 13) the similarity in the predicted dipole moment values for the small basis set CB and the extended basis set EB27 wavefunctions.

In relation to the dipole moment sensitivity to the non-relativistic 5f polarization functions on gold (correlating the 5d gold orbitals), it is found that upon including these functions the dipole moment is lowered by 0.07 a.u. (see Table 13). This result is very similar to the 0.11 a.u. lowering found by McLean [39] in a conventional non-relativistic ab-initio AuH

calculation.

However, there is a marked difference for the non-relativistic dipole moment magnitudes predicted, because at R=3.0 a.u. McLean's wavefunction predicts μ=1.839 a.u. [39] whereas EB20, which is formed with a comparable basis set, predicts μ=1.434 a.u. at Re.

This discrepancy can be understood by analysing the nature of the extended bases construction process for the wavefunction of AuH of Malli and Pyper [1] : Starting from a CB set found to contain the $5\bar{d}$, 5d and 6s DFAOs of gold plus the 1s DFAO of hydrogen [1], a series of calculations were performed for each STO polarization function added ($5\bar{d}'$, 5d, 6s', $6\bar{p}'$, 6p', $5\bar{f}'$, 5f' on gold and 1s', $2\bar{p}'$, 2p' on hydrogen), by varying its exponent to find an optimal molecular energy value.

In particular, the energy optimization for the relativistic $6\bar{p}'$ and 6p' polarization functions showed that the best 6p STOs (6pSL) should have an exponent of 2.75 [1] (which gives very contracted 6p orbitals with mean radius of 2.4 a.u.) and that these were also energetically better than the $6\bar{p}$ and 6p DFAOs (6pDF) of gold (with mean radii of 4.7 a.u. for $6\bar{p}$ and 5.5 a.u. for 6p). This is clearly shown in Table 13, where the energy lowerings (with respect to the predicted CB wavefunction energy) predicted by the extended basis wavefunctions using the CB orbital set plus the 6pSL or the 6pDF orbitals are 0.18 eV or 0.10 eV [1], respectively.

In this manner different extended bases were optimized, generating various AuH relativistic wavefunctions of differing accuracy. Then, the AuH non-relativistic extended basis wavefunctions were constructed as the non-relativistic limits of the corresponding relativistic wavefunctions. Thereby, the 6pSL orbital was used in the extended bases.

However it can be seen from Table 13 that the 6pSL (ζ=2.75, <r>=2.4 a.u.) is not the best non-relativistic 6p' polarization function, since the lowering in energy yield by enlarging the non-relativistic CB set with 6pDF (<r>=5.5 a.u.) is 0.19 eV and only 0.15 eV when using 6pSL. This implies that instead of the contracted 6p STOs (<r>=2.4 a.u.), the more extended 6p DFAOs (<r>=5.5 a.u.) should be included in the non-relativistic extended basis calculations, in agreement with the conventional AuH non-relativistic wavefunction of McLean [39], which included two diffuse 6p STOs of exponents ζ=1.69 (<r=3.8a.u.) and ζ=1.02 (<r>=6.4a.u.).

On the other hand, it is clear from the non-relativistic dipole moment results in Table 13 that inclusion of the 6p DFAOs in the extended basis wavefunctions will predict larger dipole moments, since already the predicted dipole moment value by the non-relativistic {CB+6pDF} wavefunction at Re is 1.925 a.u., which is 0.552 a.u. larger than that predicted by the non-relativistic CB wavefunction. Moreover, this result is in better agreement with the AuH conventional dipole moment value of 1.839 a.u. predicted by Mclean's non-relativistic

wavefunction [39].

3.2.3 Dipole Moments and Virial Ratios for the Chemical Basis Wavefunctions of HgH^+, TlH, PbH^+ and BiH.

The relativistic and non-relativistic expectation values for the dipole operator and for the mass operator were calculated for the systems HgH^+, TlH, PbH^+ and BiH, by using the chemical basis (CB) wavefunctions found in section 3.1. The virial ratios were computed according to eq. 55 using the total energies reported in section 3.1 and the corresponding mass operator values. The results are presented in Table 14, which also includes the dipole moment results of the CB wavefunctions of AuH given in the previous subsection.

As can be seen for the calculated dipole moment results for each species in the series, there is a clear difference between the relativistic and the non-relativistic limit predicted magnitudes.

For AuH and HgH^+, the predicted relativistic dipole moment values are smaller than the non-relativistic limit ones, whereas for TlH, PbH^+ and BiH they are larger. The relativistic dipole moment values indicate a polarity X^+H^- for all the species, however, the non-relativistic limit calculation on TlH shows the opposite polarity Tl^-H^+.

Moreover, for the series of molecules AuH, TlH and BiH, both relativistic and non-relativistic dipole moment predictions show the same trend. However, the non-relativistic predictions show

TABLE 14. Dipole Moments and Virial Ratios for the Systems AuH, HgH^+, TlH, PbH^+ and BiH calculated by using the Chemical Basis Wavefunctions at R=Re(exptl)[a].

	μ(a.u.[b])		<E>/<M>	
	Rel	NRel	Rel	NRel
AuH	0.976	1.372	1.000104	1.000411
HgH^+	3.799	4.555	1.000058	1.000056
TlH	0.323	-0.050[c]	1.000002	1.000034
PbH^+	3.675	3.580	1.000010	1.000057
BiH	0.371	0.019	0.999988	1.000054

[a] All dipoles were calculated at the experimental separation of each system except for PbH^+ where R=3.5884a.u..
[b] 1a.u.=2.54177D
[c] Negative value indicates an A^-B^+ polarity.

more drastic changes on going from the μ=1.372 a.u. of AuH to an almost non-polar BiH molecule with μ=0.019 a.u. Nevertheless, it should be noted that the above assertions for TlH and BiH must be taken carefully, since their predicted dipole moments are small and it may well be that their experimental values are of opposite sign, as was found in the calculation of the dipole moment of the CO molecule [36].

From the calculated virial ratios shown in Table 14, it is clear that the relativistic wavefunction for each system and its corresponding non-relativistic limit have nearly the same accuracy.

However, the most interesting result is that for AuH the non-relativistic virial ratio has the larger deviation from unity. Because of this, and in connection with the dipole moment discussion (see 3.2.3)), indicating that the chemical basis

should include the non-relativistic 6p DFAOs of Au, the virial ratio of the wavefunction {CB+6pDF} was calculated and a value of 1.000049 a.u. was found. This result, which gives a smaller deviation from unity and is in better agreement with the other virial ratios, confirms the importance of the 6p DFAOs for the non-relativistic AuH wavefunction.

In contrast, the virial ratio of the relativistic wavefunction with an enlarged CB set including the $6\bar{p}$ and 6p DFAOs, {CB+6pDF}, was found to be 1.000083 a.u., which is not different from the 1.000104 a.u. already calculated using the CB wavefunction, whence the minor role of the $6\bar{p}$ and 6p DFAOs in the bonding of AuH [1] is also confirmed.

4. CONCLUSIONS

In conclusion, the results presented in section 3 for the chemical basis set (CB) wavefunctions indicate that the $5\bar{d}$ and 5d DFAOs are involved in the bonding of HgH^+, whereas they do not play a significant role in TlH and PbH^+. The $6\bar{p}$ and 6p DFAOs, unoccupied in the isolated Hg^+ ion, play a more important role in the bonding of HgH^+ than the corresponding $6\bar{p}$ and 6p DFAOs of gold in the gold hydride molecule.

Moreover, the relativistic CB wavefunctions predict HgH^+, TlH and PbH^+ to be bound. In contrast, the non-relativistic limit CB wavefunctions predict HgH^+ and BiH to be unbound and TlH and PbH^+ bound. However, the predicted dissociation energies for TlH^+ and PbH^+ are almost 1 eV larger than those predicted by the corresponding relativistic CB wavefunctions.

Finally, the predicted relativistic dipole moments for the CB wavefunctions of AuH and HgH^+ are about 2 debyes smaller than the corresponding non-relativistic limit values. However, for TlH, PbH^+ and BiH, the predicted relativistic values are larger. In particular for TlH, the relativistic and non-relativistic limit CB wavefunctions predict dipole moments differing in sign and for BiH, altough the non-relativistic CB wavefunction predicted dipole moment indicates an almost non-polar system, the corresponding relativistic value indicates a polar Bi^+H^- system.

APPENDIX 1. One Centre Dipole Moment Integrals.

a) Centred at A.

The dipole moment integral has the form:

$$\langle u_A \kappa m | z_A | u'_A \kappa' m' \rangle = \int_0^\infty \left(\frac{P}{r_A} \langle l \tfrac{1}{2} j m |, -i \frac{Q}{r_A} \langle (l+a) \tfrac{1}{2} j m | \right) \times$$

$$\times \begin{pmatrix} r_A \hat{C}_{10} & 0 \\ 0 & r_A \hat{C}_{10} \end{pmatrix} r_A^2 dr_A = \begin{cases} \langle l \tfrac{1}{2} j m | \hat{C}_{10} | l' \tfrac{1}{2} j' m' \rangle \int_0^\infty r_A PP' dr_A \\ + \\ \langle (l+a) \tfrac{1}{2} j m | \hat{C}_{10} | (l'+a') \tfrac{1}{2} j' m' \rangle \int_0^\infty r_A QQ' dr_A \end{cases} \qquad (A.1)$$

Applying the Wigner-Eckart theorem:

$$\langle u_A \kappa m | z_A | u'_A \kappa' m' \rangle =$$

$$= (-1)^{j-m} (2j+1)^{1/2} \begin{pmatrix} j & 1 & j' \\ -m & 0 & m' \end{pmatrix} \times \begin{cases} \langle l \tfrac{1}{2} j \| \hat{C}_1 \| l' \tfrac{1}{2} j' \rangle \int_0^\infty PP' r_A dr_A \\ + \\ \langle (l+a) \tfrac{1}{2} j \| \hat{C}_1 \| (l'+a') \tfrac{1}{2} j' \rangle \int_0^\infty QQ' r_A dr_A \end{cases} \qquad (A.2)$$

However, the tensor $\hat{C}_1$ acts only on the orbital part of the composite system orbit-spin, therefore the reduced matrix element has to be expanded in the uncoupled representation [40]

$$\langle l \tfrac{1}{2} j \| C_1 \| l' \tfrac{1}{2} j \rangle = (-1)^{j+1/2} (2j'+1)^{1/2} \begin{pmatrix} j & j' & 1 \\ \frac{1}{2} & -\frac{1}{2} & 0 \end{pmatrix}, \qquad (A.3)$$

which is independent of l and l', therefore

$$\langle u_A \kappa m | \hat{z}_A | u'_A \kappa' m' \rangle = (-1)^{j-m+j'+\frac{1}{2}} (2j+1)^{\frac{1}{2}} (2j'+1)^{\frac{1}{2}} \times \tag{A.4}$$

$$\times \begin{pmatrix} j & 1 & j' \\ -m & 0 & m' \end{pmatrix} \begin{pmatrix} j & j' & 1 \\ \frac{1}{2} & -\frac{1}{2} & 0 \end{pmatrix} \int_0^\infty (PP'+QQ') r_A dr_A = d^1(m,m',j,j') \int_0^\infty (PP'+QQ') r_A dr_A ,$$

where d^1 is an angular coefficient introduced by Grant [41] and has the parity selection rule [23]:

$$d^1(m,m',j,j') = 0 \quad \text{unless} \quad (j+j'+1) \text{ is} \begin{cases} \text{even if } a \neq a' \\ \text{odd if } a = a' \end{cases} \tag{A.5}$$

(b) Centred at B.

For DFAOs centred at B, using $z_A = z_B + R$ gives the form:

$$\langle u_B \kappa m | \hat{z}_A | u'_B \kappa' m' \rangle = \langle u_B \kappa m | \hat{z}_B | u'_B \kappa' m' \rangle + R \delta_{\kappa\kappa'} \delta_{mm'}$$

$$= d^1(m,m',j,j') \int_0^\infty (PP'+QQ') r_B dr_B + R \delta_{\kappa\kappa'} \delta_{mm'} \tag{A.5}$$

APPENDIX 2. Dipole Moment and Mass Operator Two-centre integrals.

The radial part of the large and small component functions of the central field orbitals (eq. 2) are computed numerically by the MCDF programme which tabulates these functions at a finite number of points (about 350), equally spaced on a logarithmic grid of step size h.

Introducing the logarithmic coordinates on which r_A and r_B (see fig 1) are based:

$$r_q = r_o\, e^{h t_q} \quad , \quad q = A, B \, , \tag{A.6}$$

where r_o is the first value of r (usually 10^{-5}a.u.) at which the radial functions are computed and t is an integral parameter ($1 \le t \le 350$), the two-centre dipole moment integrals I_d (eq. 48) and mass operator integrals I_M (eq. 54) are given by

$$I = 2\pi \delta_{mm'} \int_{-\infty}^{\infty} \int_{t_A^-}^{t_A^+} G\Theta \, dt_A \, dt_B \, , \tag{A.7}$$

where

$$G = f(r_A)\, g(r_B)\, \textcircled{H}_{\ell}(\theta_A)\, \textcircled{H}_{\ell'}(\theta_B)\, \frac{r_A r_B}{R} \tag{A.8}$$

$$\Theta = \begin{cases} r_A \cos\theta_A & \text{for } I_d \\ 1 & \text{for } I_m \end{cases} \tag{A.9}$$

and

$$t_A^{\pm} = \frac{1}{h} \ln \left| \frac{R \pm r_B(t_B)}{r_o} \right| \, . \tag{A.10}$$

Unfortunately, the integral A.8 is not symmetrical in the coordinates t_A and t_B and using this form as basis for numerical integration would give unreliable results for regions near centre A [20]. This problem is solved by splitting the integration range into several symmetric areas [20]:

$$I = \int_{-\infty}^{t_c}\int_{t_A^-}^{t_A^+} G\Theta\, dt_A\, dt_B + \int_{t_c}^{\infty}\int_{t_B}^{t_A^+} G\Theta\, dt_A\, dt_B + \int_{-\infty}^{t_c}\int_{t_B^-}^{t_B^+} G\Theta\, dt_B\, dt_A + \int_{t_c}^{\infty}\int_{t_A}^{t_B^+} G\Theta\, dt_B\, dt_A , \tag{A.11}$$

where

$$t_c = \frac{1}{h}\ln\left(\frac{1}{2r_0}\right) \tag{A.12}$$

is the point corresponding to $r_A = r_B = R/2$ and

$$t_B^{\pm} = \frac{1}{h}\ln\left|\frac{R \pm r_A(t_A)}{r_0}\right| . \tag{A.13}$$

The integrals (A.11) are solved numerically using a 24x24 Gauss Quadrature [29] and to simplify the integrations, the symmetric pairs are calculated simultaneously by noting that

$$\int_a^b\int_{f_1(t_B)}^{f_2(t_B)} G\Theta\, dt_A\, dt_B = \int_a^b\int_{f_1(t_A)}^{f_2(t_A)} G'\Theta'\, dt_B\, dt_A , \tag{A.14}$$

where

$$G'\Theta' = \text{phase} \cdot G\Theta \tag{A.15}$$

and

$$\text{phase} = \begin{cases} (-1)^{(\ell+\ell'+1)-(m+m')} & \text{for } I_d \\ (-1)^{(\ell+\ell')-(m+m')} & \text{for } I_M \end{cases} \tag{A.16}$$

The phase factor appears because the change of variable $t_A \rightarrow t_B$ in log-space accounts for the inversion $z \rightarrow -z$ in cartesian coordinates that transforms $\theta_A \rightarrow \pi - \theta_B$ and viceversa.

REFERENCES

[1] Malli, G.L. and Pyper, N.C., Proc. R. Soc. Lond. A 407 , 377-404(1986).

[2] Malli, G.L. (ed) Relativistic Effects in Atoms, Molecules and Solids, NATO Series vol 87, Plenum Press (1983).

[3] Desclaux, J.P., Computer Phys. Commun., 9, 31 (1975).

[4] Grant, I.P., Computer Phys. Commun., 11, 397 (1976).

[5] Malli, G.L. and Oreg, J., J. Chem. Phys. 63, 830(1975).

[6] Malli, G.L. and Oreg, J., Chem. Phys. Letts.,9, 313 (1980).

[7] Pyykko, P. and Desclaux, J.P., Chem. Phys. Letts., 42 ,545 (1976).

[8] Pyykko, P., J. Chem. Soc. Faraday II 75, 1256 (1979).

[9] Christiansen, P.A., Lee, Y.S. and Pitzer, K.S., J. Chem. Phys.,71, 4455 (1979).

[10] Pitzer, K.S., and Christiansen, P.A., Chem. Phys. Letts., 77, 589 (1981).

[11] Hay, P.J., Wadt, W.R., Kahn, L.R., and Bobrowicz, F.W., J. Chem. Phys., 69, 984 (1978).

[12] Snijders, J.G. and Baerends, E.J., Mol. Phys.,36, 1789 (1978).

[13] Ziegler, T., Snijders, J.G. and Baerends, E.J., J. Chem. Phys.,74, 1271 (1980).

[14] Pyper, N.C., Mol. Phys.,39, 1327 (1980).

[15] Ishikawa, Y. and Malli, G.L., J. Chem. Phys.,75, 5423 (1981).

[16] Pyper, N.C. and Marketos, P., Mol. Phys.,42, 1073 (1980).

[17] Wood, C.P., and Pyper, N.C., Chem. Phys. Letts.,84 , 614 (1981).

[18] Pyper, N.C., Phil. Trans. R. Soc. Lond. A 304, 567 (1982).

[19] Wood, C.P., PhD. dissertation, Cambridge University (1984)

[20] Wood, C.P. and Pyper, N.C., Phil. Trans. R. Soc. Lond. A 320, 71-106 (1986)

[21] Roothaan, C.C.J., Rev. Mod. Phys. 23, 69 (1951).

[22] Grant, I.P., McKenzie, B.J., Norrington, P.H., Mayers, D.F. and Pyper, N.C., Computer Phys. Commun., 21, 207 (1980).

[23] Grant, I.P., Adv. Phys. 19, 747 (1970).

[24] Brown, G.E. and Ravenhall, D.G., Proc. R. Soc. Lond. A 208, 552 (1951).

[25] Sucher, J., Int. J. of Quantum Chem., 25, 3 (1984).

[26] McWeeny, R., Proc. R. Soc. Lond., A 253, 242(1959).

[27] Steiner, E., The determination and interpretation of molecular wavefunctions, Cambridge University Press, (1976), p.45.

[28] Oreg, J. and Malli, G.L., J. Chem. Phys. 61, 4349(1974).

[29] Hartree, D.R., Numerical Analysis, Oxford University Press, (1952), p.120.

[30] Kim, Y., Phys. Rev., 154, 17(1967).

[31] Steiner, E. The determination and interpretation of molecular wavefunctions, Cambridge University Press, (1976), p.113.

[32] Malli, G.L., and Pyper, N.C., private communication.

[33] Huber, K.P. and Herzberg, G., Molecular Spectra and

Molecular Structure IV, Constants of Diatomic Molecules, Van Nonstrand Reinhold, New York, (1979)

[34] Krauss, M., Stevens, W.J. and Basch, H., J. Comp. Chem. 6, 287 (1985).

[35] Cade, P.E. and Huo, W.M., J. Chem. Phys. 45, 1063 (1966).

[36] Huo, W.M., J. Chem. Phys. 43, 624(1965)

[37] Orgel, L.E., J. Chem. Soc., 4186(1958).

[38] Malli, G.L., private communication.

[39] McLean, A.D., J. Chem. Phys., 79, 3392(1983).

[40] Brink, D.M. and Satchler, G.R., Angular Momentum, Oxford University Press, (1968), p.81.

[41] Grant, I.P., Proc. R. Soc. A 262, 555(1961).

[42] Steiner, E. The determination and interpretation of molecular wavefunctions, Cambridge University Press, (1976), p.56.

[43] Grant, I.P., Mayers, D.F. and Pyper, N.C., J. Phys. B 9 , 2777 (1976).

[44] Rose, S.J., Grant, I.P., and Pyper, N.C., J. Phys. B 11 , 1171 (1978).